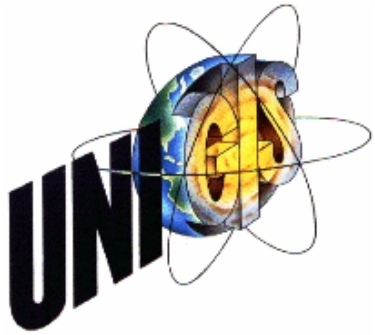

Master Thesis

im Rahmen des
Universitätslehrganges „Geographical Information Science & Systems“
(UNIGIS MSc) am Zentrum für GeoInformatik (Z_GIS)
der Paris Lodron-Universität Salzburg

zum Thema

„Sensitivity analysis of GeoWepp model regarding DEM’s spatial resolution“

vorgelegt von

Dipl. Ing. Christian Rauter

u1207, UNIGIS MSc Jahrgang 2005

Zur Erlangung des Grades
„Master of Science (Geographical Information Science & Systems) – MSc(GIS)”

Gutachter:
Ao. Univ. Prof. Dr. Josef Strobl

Wien, 04.01.2007

Meinen herzlichen Dank für die vielfältige Unterstützung an Petra!

Disclaimer

The author, Christian Rauter, clearly states that the presented thesis was written by himself using no other means than referenced.

Hiermit erkläre ich, Christian Rauter, dass ich die vorliegende Arbeit selbstständig verfasst und keine anderen als die angegebenen Hilfsmittel verwendet habe.

Vienna, 25.01.2007

Abstract and "Kurzfassung"

Abstract

This study presented the application of GeoWEPP model in an agriculturally used 22.3ha large watershed in Mistelbach - Lower Austria. The sensitivity analysis regarding the spatial resolution of the digital elevation model was conducted as follows: a native digital elevation model of 10m spatial resolution was considered as best available representation of landscape apparent at the investigated watershed. This native digital elevation model was resampled by applying nearest neighbor method, inverse distance weights method and ordinary kriging method resulting in digital elevation models with spatial resolutions of 20m, 15m, 7.5m, 5m and 2.5m. GeoWEPP was run for all 16 watershed models and simulation results of the watershed model including the native digital elevation model were compared against simulation results derived from watershed models including resampled digital elevation models. Parameters of interest were slope values derived by TOPAZ, runoff and sediment yield on hillslope and watershed level, area affected by erosion and deposition processes as well as the default classification according to the applied tolerable soil loss value underlying the visualization of spatial erosion and deposition pattern.
The results showed that GeoWEPP offers an attractive way for simulating soil erosion processes caused by water. Despite all the attractiveness of this erosion simulation approach the spatial resolution of the incorporated digital elevation model as well as the applied resampling strategy showed remarkable influence on calculated simulation results. This leads to the conclusion that the spatial resolution of the digital elevation model together with the selection of an appropriate resampling strategy in combination with an observant parameterization of the chosen resampling methodology should be taken into serious account by the application of this erosion simulation approach.

Kurzfassung

Im Zuge dieser Arbeit wurde das GeoWEPP-Modell für ein im niederösterreichischen Ort Mistelbach gelegenes und landwirtschaftlich genutztes, etwa 22.3ha großes Einzugsgebiet angewandt. Die durchgeführte Sensitivitätsanalyse betreffend der räumlichen Auflösung des verwendeten digitalen Höhenmodells wurde folgend umgesetzt: ein verfügbares digitales Höhenmodell mit einer räumlichen Auflösung von 10m wurde als beste verfügbare Repräsentation der Topographie des Einzugsgebiets definiert. Die räumliche Auflösung des Ausgangshöhenmodells wurde anschließend durch die Anwendung der Nearest Neighbor Methode, Inverse Distance Weight Methode und der Ordinary Kriging Methode erhöht bzw. verkleinert, sodass Höhenmodelle mit einer räumlichen Auflösung von 20m, 15m, 7.5m, 5m und 2.5m verfügbar wurden. Die durch das GeoWEPP-Modell berechneten Simulationsergebnisse - einerseits abgeleitet aus dem Einzugsgebietsmodell, welches u.a. aus dem ursprünglichen Höhenmodell

gebildet wurde und anderseits aus den Einzugsgebietsmodellen, welche u.a. aus den interpolierten Höhenmodellen gebildet wurden - wurden miteinander verglichen.

Der durchgeführte Vergleich umfasste die Parameter Gefälle (durch TOPAZ berechnet), den Oberflächenabfluss und Sedimentertrag unter Einzelhang- bzw. Einzugsgebietsbetrachtung, die Berechnung der von Erosions- und Depositionsprozessen betroffenen Fläche, sowie die Visualisierung der räumlichen Verteilung der Erosions- bzw. Depositionsflächen basierend auf der Klassifizierung des programmseitig vordefinierten tolerierbaren Bodenabtrags.

Die Arbeit zeigte, dass GeoWEPP eine einfach zu handhabende Möglichkeit bietet, um durch Wasser verursachte Erosionsprozesse zu simulieren. Die einfache Handhabung soll aber nicht über den beobachteten Einfluss, der räumlichen Auflösung des verwendeten Höhenmodells als auch des Einflusses der verwendeten Interpolationsmethode auf die Simulationsergebnisse hinwegtäuschen. Die gemachten Beobachtungen legen den Schluss nahe, dass die räumliche Auflösung des digitalen Höhenmodells sowie die Auswahl einer angemessenen Interpolationsmethode inklusive sorgfältiger Parametrisierung selbiger bei der Anwendung dieses Simulationsmodells gewissenhaft mitberücksichtigt werden sollten.

Table of Content

List of Figures

List of Tables

List of Abbreviations and Acronyms

BOKU	*University of Natural Resources and Applied Life Sciences*
CEC	*Cation Exchange Capacity*
CSA	*Critical Source Area*
DEM	*Digital Elevation Model*
EEA	*European Environmental Agency*
GeoWEPP	*Water Erosion Prediction Project Model incorporating GIS Technology*
GIS	*Geographic Information System*
GUI	*Graphical User Interface*
IDW	*Inverse Distance Weight Method*
IHLW	*Institute of Hydraulics and Rural Water Management*
LAI	*Leaf Area Index*
LFS	*Agricultural School (Landwirtschaftsfachschule)*
MAE	*Mean Absolute Error*
MSCL	*Minimum Source Channel Length*
MSE	*Mean Squared Error*
NN	*Nearest Neighbor Method*
OFE	*Overland Flow Element*
OK	*Ordinary Kriging Method*
WEPP	*Water Erosion Prediction Project*
TOPAZ	*Topographic Parameterization*
T-Value	*Tolerable Soil Loss Value*

Chapter 1

General Introduction

1.1 Problem Statement

Soil fulfils a wide range of environmental functions (Lal, 1997) including the production of food, fuel, fibre and building materials as well as the production of biomass for industrial use. Additionally, soil is used as retention of large gen pool, for environmental regulation, engineering and military use, aesthetic and cultural use and it serves the archeological function. The performance of these environmental functions as well as the capacity to produce economic goods and services is closely related to soil quality.

Soil degradation (Lal, 1997) is linked to the decline in soil quality thus a reduction in productivity and environmental regulatory capacity caused by the impact of anthropogenic or natural factors.

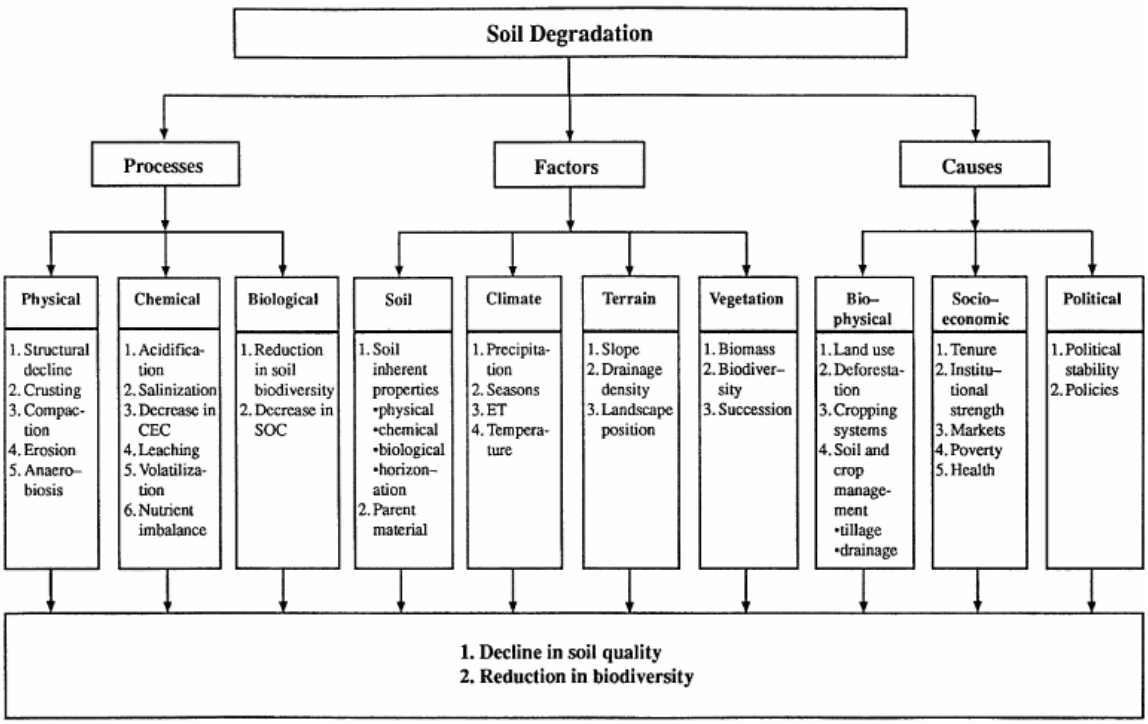

Figure 1.1: Soil degradation (source: Lal, 1997)

Soil degradation processes are threesome (Lal, 1997): physical, chemical and biological. The decline in soil structure is one of the most important among the group of physical processes. This decline leads to crusting, compaction, erosion, desertification, anaerobiosis, environmental pollution

and an unsustainable use of natural resources. The chemical processes comprehend acidification, leaching, salinization, reduction in cation exchange capacity (CEC) and loss of fertility. Finally the biological processes include a decline in biodiversity and a reduction in total and biomass carbon.

European Environmental Agency (EEA, 2003) argues that soil erosion in Europe became the major and most widespread form of land degradation effecting about 17% of total land area, whereby wind erosion shows minor influence compared to erosion caused by water which is seen as the main erosion type in about 92% of outlined area.

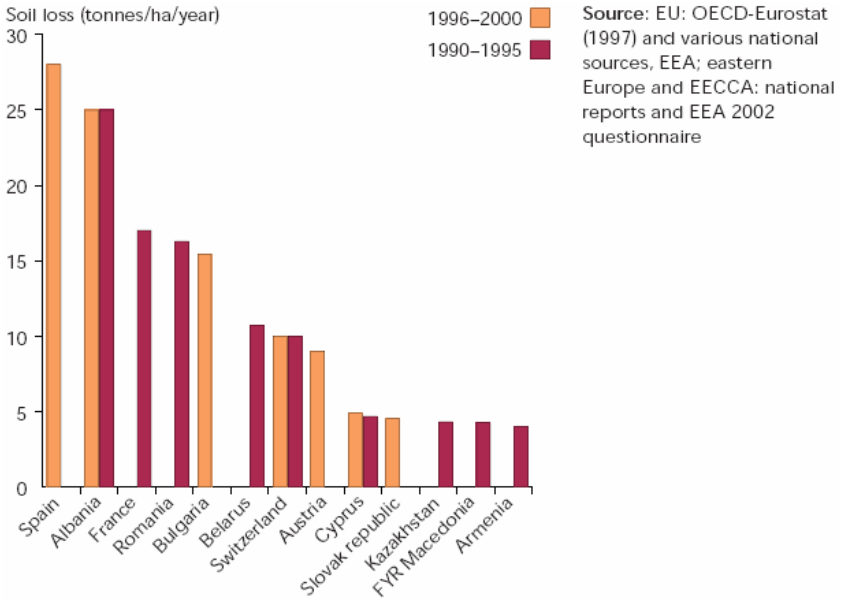

Figure 1.2: Annual soil loss in agricultural land by erosion (source: EEA, 2003)

Regarding the magnitude of soil loss (Figure 1.2) and the slow process of soil formation, any soil loss greater than 1 tonne/ha/year can be considered as irreversible within a time span of 50-100 years (EEA, 2003). Despite this irreversibility aspect, costs of about 53 EUR/ha for on-site effects of soil erosion and off-site effects of about 32 EUR/ha (EEA, 2003) yields major economic consequences of soil erosion.

Considering these numbers, the need for environmental assessment and management tools becomes obvious. Scientists and engineers approach the study of an environmental system (Renschler, 2003) especially its inherit behavior as well as its reaction to natural and anthropogenic changes by describing environmental processes and environmental properties at a spatial and temporal scale of interest and by parameters, equations and possibly within a process based environmental model.

This model can be used as a basis for decision making, as well as the design of specific environmental management practices (Renschler, 2005). Common to all models is that they were

designed to address specific questions at a specific temporal and spatial scale range and with data of known quality. This context justifies necessary explicit or implicit assumptions in model design, calibration and validation (Renschler, 2003).

Nowadays various erosion models (conceptual, empirical and physical based models) are available (Figure 1.3). Process based models theoretically need a minimum of calibration, reflect detailed scientific knowledge of environmental processes and properties at a very fine spatial and temporal scale and therefore require extensive input data. Empirical models on the other hand are easier to apply, need less input data, therefore do not take the full advantage of scientific process understanding and have limited applicability outside their development context (Renschler, 2003).

Model	Type*	Scale	Input/output	Reference
Water quality				
AGNPS	Conceptual	Small catchment	Input requirements: High Output: runoff volume; peak rate, SS, N, P, and COD concentrations	Young et al. (1987)
ANSWERS	Physical	Small catchment	Input requirements: High Output: sediment, nutrients	Beasley et al. (1980)
CREAMS	Physical	field 40–400 ha	Input requirements: High Output: erosion; deposition	Knisel (1980)
EMSS	Conceptual	Catchment	Input requirements: Low Output: runoff, sediment loads, nitrogen loads and phosphorus loads	Vertessey et al. (2001) Watson et al. (2001)
HSPF	Conceptual	Catchment	Input requirements: High Output: runoff, flow rate, sediment load, nutrient concentration	Johanson et al. (1980)
IHACRES-WQ	Empirical/ Conceptual	Catchment	Input requirements: Low Output: runoff, sediment and nutrients	Jakeman et al. (1990, 1994a,b), Dietrich et al. (1999)
IQQM	Conceptual	Catchment	Input requirements: Moderate Output: many pollutants including nutrients, sediments, dissolved oxygen, salt, algae.	DLWC (1995)
LASCAM	Conceptual	Catchment	Input requirements: High Output: runoff, sediment, salt fluxes	Viney and Sivalapan (1999)
SWRRB	Conceptual	Catchment	Input requirements: High Output: streamflow, sediment, nutrient and pesticide yields	USEPA (1994)
Erosion				
GUEST	Physical	Plot	Input: High Output: runoff; sediment concentration	Yu et al. (1997) Rose et al. (1997)
LISEM	Physical	Small catchment	Input: High Output: runoff; sediment yield	Takken et al. (1999) De Roo and Jetten (1999)
PERFECT	Physical	Field	Input: High Output: runoff, erosion, crop yield	Littleboy et al. (1992b)
SEDNET	Empirical/ Conceptual	Catchment	Input requirements: Moderate Output: suspended sediment, relative contributions from overland flow, gully and bank erosion processes	Prosser et al. (2001c)
TOPOG	Physical	Hillslope	Input: HighOutput: water logging, erosion hazard, solute transport	CSIRO Land and Water, TOPOG Homepage; Gutteridge Haskins and Davey (1991)
USLE	Empirical	Hillslope	Input: High Output: erosion	Wischmeier and Smith (1978)
WEPP	Physical	Hillslope/ catchment	Input: High Output: runoff; sediment characteristics; form of sediment loss	Laflen et al. (1991)
In-stream transport				
MIKE-11	Physical	Catchment	Input: High Output: sediment yield, runoff	Hanley et al. (1998)

Figure 1.3: Erosion and sediment transport models - overview (Merrit et. al, 2003)

Regarding the questions asked in the context of soil erosion (Boardman, 2006) these models can help by providing answers to these questions. Indirectly incorporated into these questions is the need for further model improvement and development.

Table 1.1: Big questions and issues according to Boardman (2006)

Questions		Issues
Where is erosion happening?		Scale
	— Global hotspots	Datasets
Why is it happening?		Causality
	— The big picture: socio-economic drivers	
	— The details: runoff, wind, soil etc	
When is it happening?		Temporality
	— Change through time, seasonality, climate	
Who is to blame?		Responsibility
	— Farmers driven by policy imperatives at national and local scales	
How serious is it?		Impacts
	— Magnitude, frequency	
Who does it affect?		Economics
	— On and off-site impacts	
What does it cost?		
	— Short and long term costs	
	— Agricultural externalities	
Over what time scale is degradation occurring?		Sustainability
	— Threat to agriculture and livelihoods	
Can we do anything about it?		Response
	— Effectiveness of conservation	
Who should take action?		
	— Farmers; local, national government	
Is action worthwhile?		Ethics and economics
What is the risk of erosion in the future?		Prediction
	— Land use and/or climate change	
Where is that risk?		
	— Vulnerable soils, vulnerable communities	

Nearing (2006) states that appropriately applied models are valuable tools for decision makers for the following reasons:

- support the land owners by the process of choosing suitable conservation practices
- help estimating long-term loadings to water bodies
- can be applied as a storm response design tool
- can be used to conduct broad-scale erosion surveys

The decision maker is confronted with three concurrent initial steps when choosing an appropriate model (Renschler, 2003). Firstly by selecting the scale of interest (assessment results), secondly with availability of data sets that support a proper model application (assessment base) and thirdly with the model choice that adequately represents decision making goals (assessment core).

Due to the variety of models for a single or similar environmental process, the actual model selection is based on user friendliness, model appearance, system requirements, input data availability and past use (Renschler, 2005). These selection criteria may include the necessity of model scaling because the model developers intention, especially the spatial and temporal range of scale and the known data quality, might differ from those of the decision makers context.

The availability of free geo-spatial model input data (especially in the U.S.), the increased performance of home computers and the availability of GIS systems for geo-spatial data assembling, storage, analysis and visualization extends the model users from solemnly scientific users towards application-oriented users as there are planners, farmers, politicians and environmental groups (Renschler, 2003).

In this study GeoWEPP model is applied to simulate erosion and deposition processes in a 22.3ha large agriculturally used watershed in Lower Austria with the main objective of investigating consequences on simulation results caused by the change of spatial resolution incorporated in the used digital elevation model. The GeoWEPP approach is based on the WEPP model (Water Erosion Prediction Project) (Flanagan and Nearing, 1995) and incorporates GIS technology as well as the hillslope and watershed technology of WEPP. This approach provides a graphical user interface (GUI) that allows anybody an easy handling of the necessary modeling steps.

1.2 Motivation and research questions of this study

The previously provided concept of the GeoWEPP approach namely the increase of potential model user in combination with a straight forward model application approach, considering an accurate simulation run, always leads to simulation results. These results are presented either as visualized on-site or off-site erosion and deposition patterns or as text files containing calculated values for further analysis. Independent of the appropriateness of the watershed or hillslope model a simulation result is achieved.

The concept of this study deals with the consequences on simulation results and follows the subsequently described thoughts. Given a digital elevation model with a native spatial resolution of 10m model user might think this resolution should be improved for erosion simulation purposes. One way of improvement is offered by the application of resampling strategies. By screening literature it becomes obvious that the topic of resampling strategies opens a wide field of possible methods. Even by selecting a theoretically suitable method the step of parameterization still remains. This necessary step again requires various decisions to achieve reasonable resampling results.

Given the continuity of landscape surface at study site nearest neighbor method is considered as one possible resampling strategy. In order to validate results derived by this method a conceptually different resampling strategy namely inverse distance weight method is selected. Additionally the conceptually similar ordinary kriging method is chosen to provide a third reference value clearly stating that the adequately application of ordinary kriging is much more sophisticated than inverse distance weight method.

Despite the question complex about the suitability of a method the question about the parameterization of any method comes into mind. Taken these three methods each one is supported by a different number of parameters. This study focuses on the consequences of a minimum adaption of defaultly provided parameters on simulation results. This assumes that model user is not too familiar with geostatistics and applies the parameter sets proposed by software with a minimum of adaption to actual circumstances.

The actually investigated spatial resolutions of digital elevation model, namely 20m, 15m, 7.5m, 5m and 2.5m should simulate consequences of fine as well as coarse spatial resolution on erosion simulation results. In order to quantify these consequences the simulation results derived from the native 10m spatial resolution DEM are considered as reference values due to the assumption of best available representation of study site's landscape and all other calculated values are compared to these values.

These reflections lead to the upcoming questions of research:

Do the selected resampling strategies affect simulation results on hillslope and watershed level equally?

What is the quantitative difference of area size affected by erosion and deposition processes within the watershed regarding applied resampling strategies and investigated spatial resolutions?

Does the magnitude of event related parameters like runoff and sediment yield vary between different spatial resolutions that are derived by different resampling strategies? Is there a different parameter behavior between hillslope and watershed level observable?

Is there any considerable change in the calculated slope by TOPAZ (topographic parameterization algorithm) regarding different spatial resolutions?

1.3 Outline of the thesis

Chapter 1 outlines the problem statement, offers an introductory overview of consequences caused by soil degradation, provides available model concepts and addresses the research questions of this study.

Chapter 2 uses a literature review to go more into detail on TOPAZ software, the erosion component of the WEPP model and finally on the GeoWEPP approach.

Chapter 3 introduces the study site regarding climate characteristics, soil types and management practices.

Chapter 4 outlines the parameterization of the investigated watershed for GeoWEPP model according the local conditions.

Chapter 5 deals with the applied resampling strategies, their theoretical background and the analysis of the estimates derived by the application of nearest neighbor, inverse distance weight and ordinary kriging method. The calculated residuals are statistically and spatially described.

Chapter 6 presents an analysis of simulation results at various spatial resolutions with focus on the magnitude of differences of area occupied by erosion or deposition processes, surface runoff and sediment yield from hillslope as well as runoff volume, peak runoff and sediment yield from watershed.

Chapter 7 summarizes the observations made during this study.

Chapter 2

Literature Review

2.1 Introduction

This literature review offers a detailed perspective on TOPAZ regarding the treatment of DEM's depressions and flat areas, the erosion component of the WEPP model and finally the GeoWEPP framework.

2.2 TOPAZ (Topographic PArameteriZation)

Topaz is a suite of FORTRAN algorithms, developed for the topographic parameterization of watersheds using a digital elevation model (DEM). The basic concepts implemented in these algorithms are the D8 method, the downslope flow routing concept and the critical source area (CSA) concept (Garbrecht and Martz, 1999). The D8 method determines the flow direction by evaluating elevation of each cell with its 8 adjacent cells. The steepest downslope path from the cell of interest to one of its 8 adjacent neighbors is used by the downslope flow routing concept to define flow direction on landscape surface. The CSA concept leads to the definition of permanent channels within the watershed. This concept represents a threshold value of drainage area for channel definition.

Topaz deals with the shortcomings of DEM in respect of closed depressions and flat areas as follows. Closed depressions and flat areas may result from inaccuracies and low spatial resolution of input data used for the generation of a DEM. They may cause problems by the automated definition of overland flow across raster DEM surfaces (Martz and Garbrecht, 1999). Topaz differentiates between sink-depressions and impoundment depressions. Sink-depressions are defined as a group of raster cells with lower elevation as surrounding landscape, while impoundment depressions are caused by a band of adjacent cells of higher elevation across drainage path comparable to a dam across flow direction (Garbrecht and Martz, 1999).

2.2.1 Depression treatment

Depressions are tackled with a three step procedure. First the identification of the depression, second the depression breaching and third the depression filling (Martz and Garbrecht 1999). The identification of depression is achieved by the location of inflow sinks, definition of sink contributing

area, evaluation of potential outlet and finally the evaluation of the depression regarding the distinction between depression and flat area. In case of flat area no breaching is applied.

The depression breaching consists of two major steps. Firstly the selection of the breaching site and secondly the breaching itself. The number of cells included in the breaching process can be defined as an input parameter of the software and can vary between zero (no breaching), one and two cells. The maximum of two cells is considered as the recognition and the remove of spurious depressions.

Finally the remaining depressions (after the breaching procedure was applied) are filled in order to remove them from the digital elevation model. This method of depression filling implies that all depressions are caused by an underestimation of elevation.

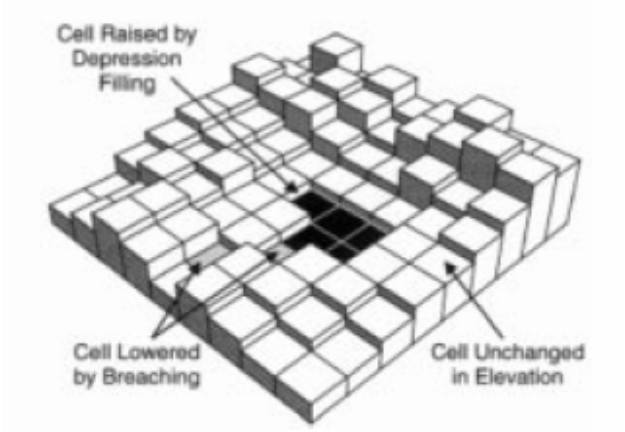

Figure 2.1: Depression handling by TOPAZ (source: Martz and Garbrecht, 1999)

2.2.2 Flat area treatment

As flat areas do not support the D8 algorithm, these areas must be addressed and corrected before the algorithm can be unambiguously applied (Garbrecht and Martz 1997). Considering that flat areas are already defined, Topaz applies a two step procedure to define flow direction on flat areas. Firstly the assumption that drainage is generally towards lower terrain is implemented by infinitesimally small increase of elevation on the flat area. The magnitude of modification is about 2/100 000 of vertical DEM resolution. This results in a gradient from higher to lower elevation. Reality is not violated by this approach but it enables the definition of flow direction on flat areas (Figure 2.2). The value in the right upper corner of the rectangulars indicates a fictive height, while the value at the lower left corner indicates the number of increments.

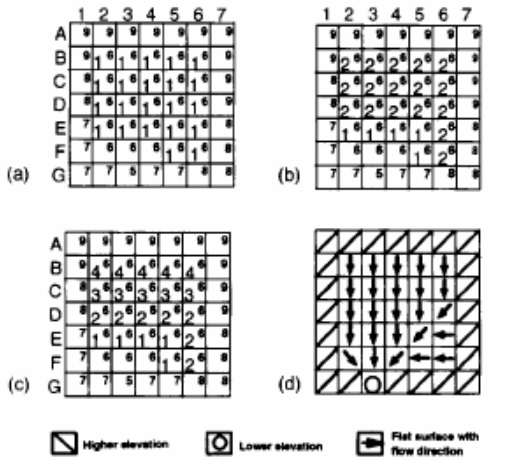

Figure 2.2: Gradient from higher to lower elevation (source: Garbrecht, 1997)

Secondly waterflow is forced away from higher terrain based on the condition that the cell of interest is adjacent to a cell of higher elevation and not surrounded by adjacent cells of lower elevation which results in a second gradient.

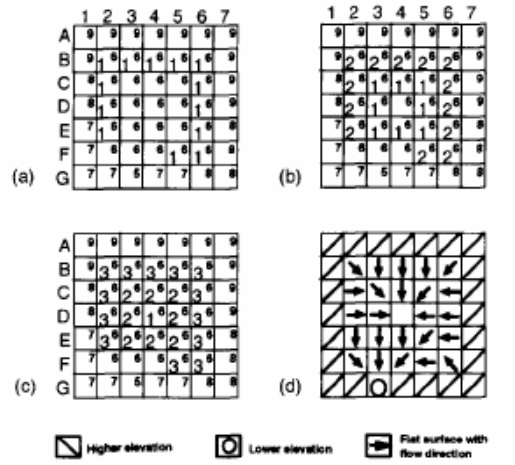

Figure 2.3: Gradient away from higher terrain (Garbrecht, 1997)

Both gradients are coded as increments on grid basis and finally the derived increments are linearly added for each cell. Regarding the resulting grid the steepest flow path can be unambiguously assigned.

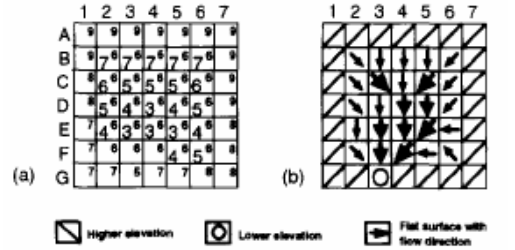

Figure 2.4: Unambiguous flow assignment (Garbrecht, 1997)

The TOPAZ application is tied to some preconditions that must be taken into consideration for a proper application (Garbrecht and Martz, 1999).

- spatial resolution must be at least twice as high as landscape features of relevance
- drainage direction for plane undissected hillslopes is prone for large approximation errors
- modeling of divergent and braided flow pattern is impossible
- landscape drainage properties associated with true depressions cannot be generated directly

2.3 WEPP[1]

The WEPP (Water Erosion Prediction Project) model (Flanagan and Nearing, 1995) is a process based erosion model that can be either run in hillslope mode or watershed mode. The model can be run on single event basis or in continuous simulation mode. Regarding continuous simulation mode Nearing (2006) states that the accuracy of simulation results is increased by an increase of the considered time span. The simulation results of soil loss, surface runoff and sediment delivery are on a daily, monthly or average annual basis in terms of temporal extend and are representative for whole hillslope profiles, interior points of the hillslope profile or for whole watershed in terms of the spatial extend.

A hillslope represents an individual unit (e.g. an agriculturally used field) with all its characteristics like slope length, gradient, soil types, management practices and numerous additional parameters. The hillslope can be divided into overland flow elements (OFEs) in order to accommodate regions of uniformity along the individual hillslope into the model. A watershed is represented by various hillslopes that are connected by cannels routing to the watershed outlet.

The following listing offers an overview of implemented processes in the WEPP model while only the interrill and rill erosion processes are covered in more detail with respect to the topic of this study. The model incorporated processes are as follows: “rill and interrill erosion, sediment transport and deposition, infiltration, soil consolidation, residue and canopy effects on soil detachment and infiltration, surface sealing, rill hydraulics, surface runoff, plant growth, residue decomposition, percolation, evaporation, transpiration, snow melt, frozen soil effects on infiltration and erodibility, climate, tillage effects on soil properties, effects of soil random roughness, and contour effects including potential overtopping of contour ridges” (Flanagan and Nearing, 1995).

2.4 Hillslope erosion component

[1] see Flanagen and Nearing (1995), Chapter 11

The movement of sediment in a rill is described with a steady-state sediment continuity equation in the WEPP hillslope erosion model (Flanagen and Nearing, 1995).

$$\frac{dG}{dx} = D_f + D_i \qquad [1]$$

where:

G = sediment load $(kg \cdot s^{-1} \cdot m^{-1})$ on a per unit rill width basis

x = distance downslope (m)

D_f = rill erosion rate $(kg \cdot s^{-1} \cdot m^{-2})$ on a per rill area basis; + for detachment, - for deposition

D_i = interrill sediment delivery $(kg \cdot s^{-1} \cdot m^{-2})$ on a per rill area basis; always positive

Interrill erosion:

The interrill erosion process delivers sediment from the interrill parts of the hillslope to a concentrated flow channel or rill. The sediment is then either carried off the hillslope by the concentrated flow or deposited in the rill (Flanagen and Nearing, 1995). The interrill erosion rate is calculated as follows:

$$D_i = K_{iadj} I_e \sigma_{ir} SDR_{RR} F_{nozzle} \left(\frac{R_S}{w} \right) \qquad [2]$$

where:

K_{iadj} = adjusted interrill erodibility

I_e = effective rainfall intensity $(m \cdot s^{-1})$

σ_{ir} = interrill runoff rate $(m \cdot s^{-1})$

SDR_{RR} = sediment delivery ratio (function of random roughness, row side-slope and interrill particle size distribution)

F_{nozzle} = irrigation adjustment factor

R_S = rill spacing (m)

w = rill width (m)

Rill erosion:

Rill detachment is observed when two criteria are met:

- hydraulic shear stress exceeds critical shear stress of the soil
- sediment load falls below sediment transport capacity

The calculation is as follows:

$$D_f = D_c \cdot (1 - \frac{G}{T_c}) \quad [3]$$

where:

D_c = detachment capacity by rill flow $(kg \cdot s^{-1} \cdot m^{-2})$

T_c = sediment transport capacity in the rill $(kg \cdot s^{-1} \cdot m^{-1})$

The transport capacity is calculated using a simplified transport equation for interior profile points and a modified form of the Yalin-equation for the end of the profile. The simplified transport equation is as follows:

$$T_C = k_t \cdot \tau_f^{3/2} \quad [4]$$

where:

k_t = transport coefficient $(m^{0.5} \cdot s^2 \cdot kg^{-0.5})$ - dependent on slope steepness

τ_f = hydraulic shear stress acting on the soil *(Pa)*

In case that first criterion is met the detachment capacity is expressed as:

$$D_c = K_r \cdot (\tau_f - \tau_c) \quad [5]$$

where:

K_r = rill erodibility parameter $(s \cdot m^{-1})$

τ_f = flow shear stress *(Pa)*

τ_c = critical shear stress of the soil *(Pa)*

With the calculation of τ_f the influence of slope angle comes into to the calculation of rill detachment because the average slope angle of a uniform slope segment is taken into account. The ratio of f_s / f_t accounts for the partitioning of shear stress in shear stress acting on the soil and total hydraulic shear stress that also includes shear stress acting on surface cover.

$$\tau_f = \gamma \cdot R \cdot \sin\alpha \cdot \frac{f_s}{f_t} \quad [6]$$

where:

γ = specific weight of water $(kg \cdot m^{-2} \cdot s^{-2})$

R = hydraulic radius (m)

α = average slope angle of the uniform slope

f_s = friction factor for the soil

f_t = total rill friction factor

Rill deposition is computed when second condition is not met. This means that sediment load exceeds the transport capacity. The computation follows the equation:

$$D_f = \frac{\beta V_f}{q} \cdot (T_c - G) \quad [7]$$

where:

V_f = effective fall velocity for the sediment $(m \cdot s^{-1})$

q = flow discharge per unit width $(m^2 \cdot s^{-1})$

β = raindrop induced turbulence coefficient ($0.5 < \beta < 1.0$)

A β value of 0.5 indicates that rill flow is impacted by rain drops, otherwise (in case of e.g. snow melting, furrow irrigation) a value of 1.0 is assigned.

2.5 GeoWEPP

GeoWEPP summarizes a package of algorithms including Avenue scripts, FORTRAN and C++ scripts in combination with ArcView GIS and WEPP. This setup facilitates the easy simulation of soil erosion for the purpose of decision making (Renschler, 2003). There are two basic simulation modes (neglecting the manual approach) that GeoWEPP can be run. On the one hand the flowpath mode where the WEPP model is run for each individual flowpath within the watershed and on the other hand the hillslope mode where flowpaths within hillslopes are transformed into representative slope profiles and slope profile lengths (Cochrane, 1999). In case of flowpath mode the erosion model is run for each individual flowpath within the watershed leading finally to a classified visualization of erosion and deposition pattern. The identification of representative slope profiles and slope profile lengths is therefore not required for this simulation mode.

2.5.1 GeoWEPP – hillslope method

The application of WEPP together with ArcView GIS and DEMs covers basically the steps of DEM preprocessing, channel and hillslope identification, definition of representative hillslopes including definition of slope profile and slope profile length respectively (Cochrane, 2003).

Watershed segmentation

TOPAZ is applied on the DEM to overcome the shortcomings of depressions and flat areas that might be included in the original DEM and to derive the segmented watershed necessary to define the representative hillslopes and channels required as WEPP input. The segmentation is based on a variety of parameters including two threshold values namely CSA (critical sources area) and MSCL (minimum source channel length) in order to delineate the watershed. The segmentation process is finished by the definition of a watershed outlet.

The CSA defines the upslope drainage area that is necessary to initiate a permanent channel where all the defined flowpaths drain into while MSCL prunes all channel links shorter than the specified threshold value before the final drainage network is defined (Martz, 1999). Among the various output files generated by TOPAZ the four files flopat.arc, flovec.arc, subwta.arc and fvslop.arc are selected to generate one file where each cell of each flowpath in a specific hillslope holds a slope value (Cochrane, 2003). This file gives the basis for further analysis in respect to the necessary WEPP input parameters.

Representative Hillslope

A representative hillslope should account for all individual flowpaths within the hillslope and reflect the effects of slope on simulated soil erosion. This requires the definition of a representative slope profile as well as a slope profile length. The transformation from TOPAZ output into a representative slope profile is achieved by a method called weighted average method while the transformation into a representative slope profile length is achieved by either the chanleng (for channel length) or the calcleng (for calculated length) method (Cochrane, 2003).

Weighted average representative slope profile

This method averages each slope value from a flowpath with all matching cells from all flowpaths within the hillslope. The matching criterion for the investigated cell is the distance from channel. This approach assumes that flowpaths with greater area and greater length contribute proportionally more to the representative slope profile than smaller flowpaths with less area and length (Cochrane, 2003).

$$E_i = \frac{\sum_{p=1}^{m} z_{pi} \cdot k_p}{\sum_{p=1}^{m} k_p} \quad [8]$$

where:

E_i = weighted slope value for all flowpaths at distance *i* from the channel

z_{pi} = slope of flowpath *p* at distance *i* from the channel

k_p = weighting factor for flowpath p

Representative slope profile length

Chanleng method

This method assumes that the hillslope width is equal to the channel length. The hillslope length is then easily calculated by dividing hillslope area by hillslope width (Cochrane, 2003). This approach works in case that the investigated hillslope is adjacent to the channel. Considering a primary channel that is laterally as well as from top drained, a different method must be applied.

Chancalc method

The length for the slope profile is calculated by averaging all flowpaths within the hillslope based on their drainage area. The hillslope width is then calculated by dividing the hillslope area by the slope profile length (Cochrane, 2003).

$$L = \frac{\sum_{p=1}^{n} l_p \cdot a_p}{\sum_{p=1}^{n} a_p} \quad [9]$$

where:

l_p = flowpath length

a_p = area represented by the cells in the flowpath

n = number of flowpaths in the hillslope

Chapter 3

Study Site Description

3.1 General description

The study site is located at municipality of Mistelbach precisely at "Schneiderberg" which is a part of Mistelbach located in the north-eastern direction seen from Mistelbach center. The study site is about 22.3ha of size and agriculturally used except a small field of about 0.9ha that is forested with acacia trees. While almost the entire northern half of the study site is cultivated by an agricultural school (LFS – Mistelbach) the southern part is privately owned. This fact is remarkable because the availability of data varies strongly between these two sources.

Figure 3.1: Location of Mistelbach study site (source: Wikipedia)

The number of values included in the computation of descriptive statistics (Table 3.1) providing information regarding elevation is 2323 for slope and 2180 for aspect. Range of study site's elevation reaches from 231.562m to 264.972m with a mean value of 251.980m (± 8.039m). Regarding the distribution of slope values especially distribution's mean and median value the majority of gradients show low values at the study site. This observation is also supported by the value of the third quartile that also indicates some areas with a high gradient. The outlined aspect

(zero points to north) values indicate a dominating aspect into the eastern towards southern direction.

Table 3.1: Terrain characteristics of study site

	Elevation (m)	Slope (°)	Slope(%)	Aspect (°)
Mean	251.980	4.596	8.1	120.8
Standard deviation	8.039	2.436	4.3	51.7
Variance	64.628	5.934	18.5	2673.5
Coefficient of variation	0.032	0.530	0.5	0.4
Minimum	231.562	0.533	0.9	27.2
First quartile	246.662	2.678	4.7	78.6
Median	253.138	4.112	7.2	112.5
Third quartile	258.597	5.963	10.4	157.2
Maximum	264.972	13.848	24.7	251.8
Range	33.410	13.315	23.7	224.6

3.2 Precipitation

Rainfall measurement data for erosion purposes optimally serves the need for data with a high temporal resolution. This request can be easily proved by the fact that intensity (amount of rainfall over a certain period of time) has a strong influence on the erosion process as well as on the calculation of rainfall related parameters.

In case of Mistelbach watershed the available temporal data resolution covers measurement intervals of 5 minutes. The measurement is executed by Ihlw-BOKU and all following figures utilize these datasource. One figure shows monthly average values for precipitation and temperature and the other shows the same parameters on a daily basis for the year 2003.

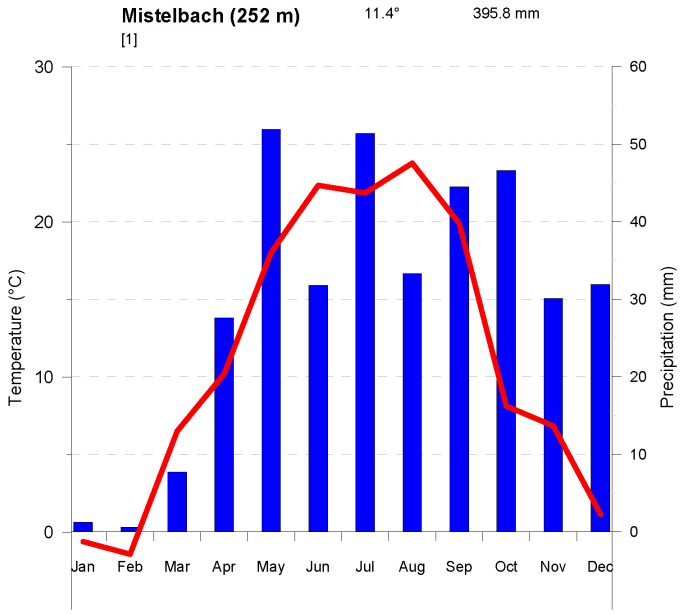

Figure 3.2: Climate diagram for Mistelbach watershed of year 2003 (data source: Ihlw-Boku)

An obvious observation regarding the first figure is the very low annual total of rain (395.8mm). Based on a 11-years time series showing an average annual total of 659mm (±129mm) the year 2003 falls about 250mm below the average.

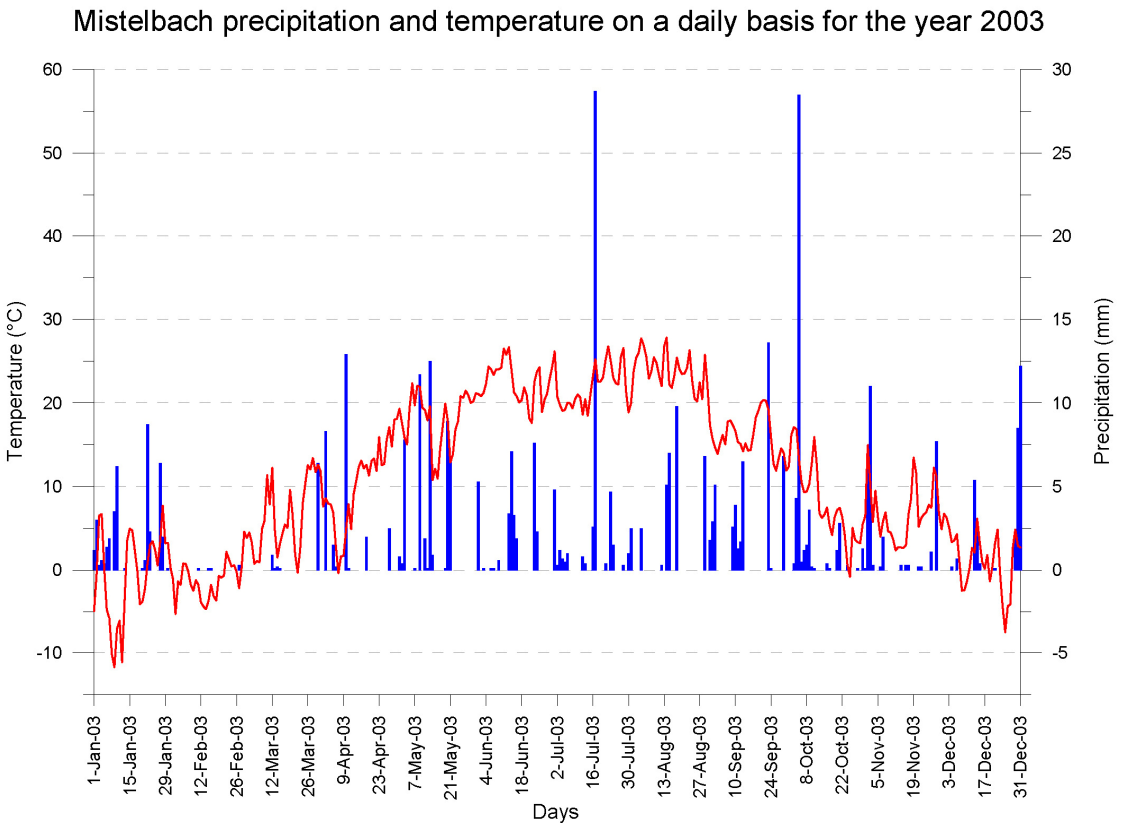

Figure 3.3: Mistelbach precipitation and temperature on a daily basis for the year 2003 (data source: Ihlw-Boku)

Considering all observed 128 storm events in 2003, Figure 3.3 outlines two storms with a remarkable high amount of rainfall compared to the other storm events through out the year 2003. On 17th of July the observed storm reached a total of 28.7mm as on 5th of October a total of 28.5mm was reached which is about 9 times the average storm total of 3.1mm (±4.6mm) for the year 2003. Classifying the rainfall amount into three classes reaching from 0.1mm to 7.5mm, from > 7.5 mm to 15 mm and from > 15 mm to 30 mm, 114 events fell into the first class, 14 fell into the second and only the two previously mentioned fell into the third class.

3.3 Soil types

The definition of soil types within Mistelbach watershed is taken from the „Amtliche Österreichische Bodenkarte M=1:25 000) and is as follows: 33 uL (0.7 %), 52 lU (0.9%), 9 sL (5.9%), 61 lU (8.5%), 13 lU (22.2%), 14 lU (23.8%) and 50 lU (38.0%) (Figure 3.4).

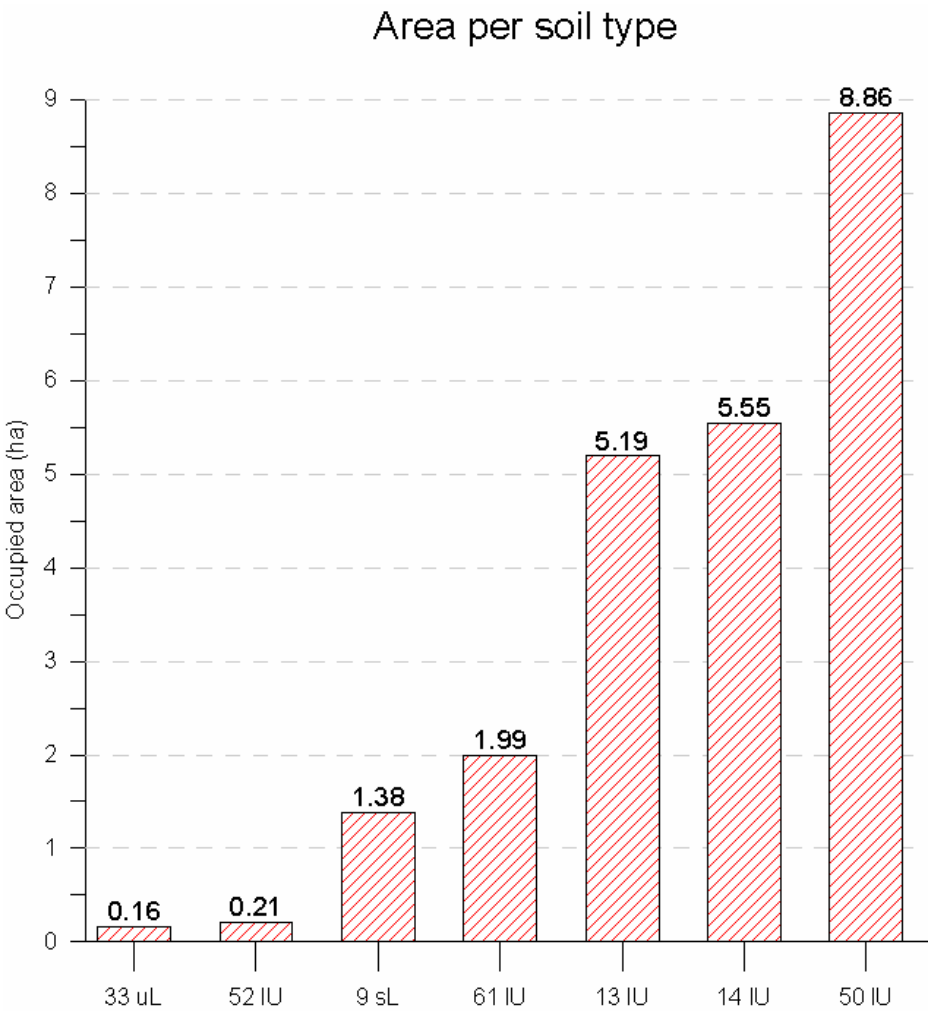

Figure 3.4: Area per soil type (data source: Ihlw-Boku)

The outlined numbers correspond with the glossary of the mentioned soil map. The characters next to the numbers characterize the components of the addressed soil type. The distribution of the contained particle fractions by an individual soil is summarized next (Table 3.2).

Table 3.2: Definition of soil types according to the Austrian soil map

Symbol	Soil type	Sand (2.000-0.060 mm)	Silt (<0.060-0.002mm)	Clay (<0.002mm)
		content in %		
sL	sandy loam	20-75	10-55	15-25
lU	loamy silt	0-30	55-75	15-25
uL	silty loam	0-20	55-75	25-45

The spatial distribution of the identified soil types within the watershed is shown in Figure 3.5. Figure 3.6 summarizes the content of organic material, sand and clay of each soil type. These parameters among others form the data basis for necessary soil input parameters of the WEPP model. They are discussed in a later chapter in more detail. The CEC (cation exchange capacity) and the content of rocks are considered constant for all different soil types.

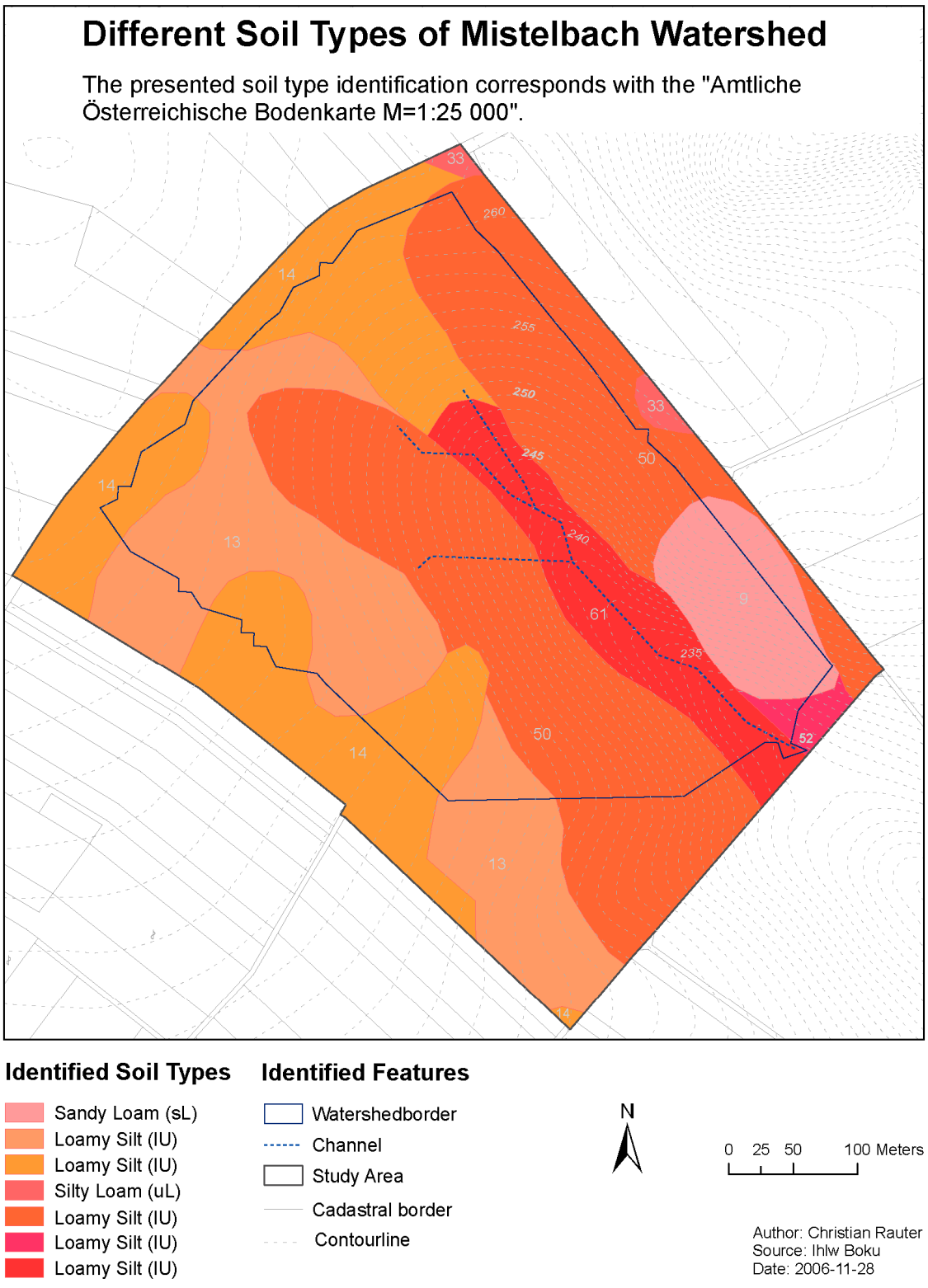

Figure 3.5: Spatial distribution of soil types (data source: Ihlw-Boku)

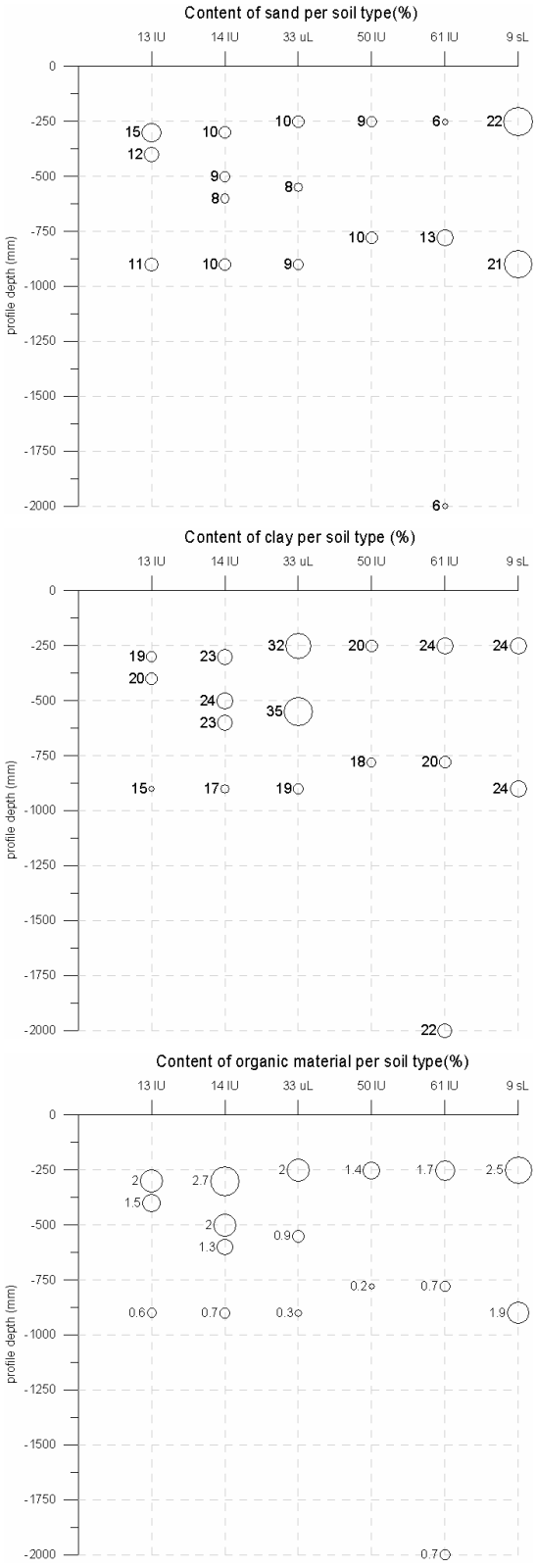

Figure 3.6: Content of selected soil parameters

3.4 Crop types

The planted crops for the year 2003 where corn (10.4%), winter wheat (31.8%), peas (8.3%), summer barley (32.2%), grass (4.8%), forest (3.8%) and canola (8.8%).

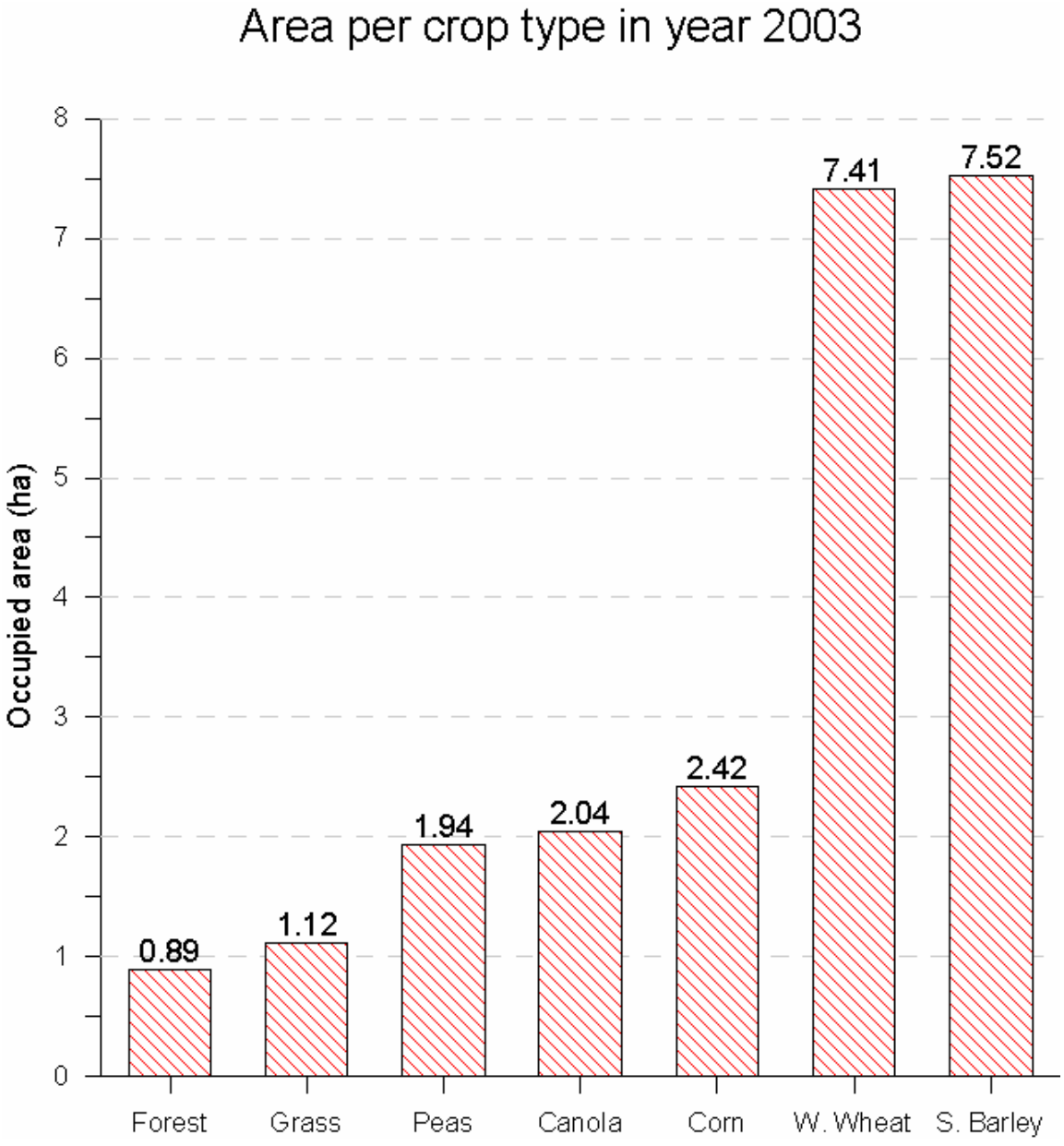

Figure 3.7: Area per crop type

The spatial distribution of the planted crop types is presented in Figure 3.8. Crop type “no crops” indicates transport paths within the watershed.

Figure 3.8: Spatial distribution of crop types (datasource: LFS - Mistelbach)

Chapter 4

WEPP Input Parameters

4.1 Climate Input

Rainfall data is measured and recorded in the field by any type of rain gauge and is characterized by the rain gauge's typical data layout. This layout does not meet the requirements of the WEPP climate file input neither with the existing kind of rainfall parameterization nor with the amount of required input parameters. Therefore the measured data has to be disaggregated and converted into a WEPP readable layout and missing parameters need to be added. Regarding the WEPP climate file layout two different layout types can be distinguished namely the no-breakpoint and the breakpoint layout type.

Both types of climate file layouts consist of two sections namely the header and the body section. While the header section is the same with both layout types, the body section varies between the no-breakpoint and the breakpoint layout.

```
3.10
  1   0   0
  Station:  DES MOINES WB AP IA                              CLIGEN VERSION 3.1
Latitude Longitude Elevation (m) Obs. Years   Beginning year  Years simulated
   41.53   -93.65         289          44           1                5
Observed monthly ave max temperature (C)
 -2.0   1.2   7.5  16.2  22.6  27.8  30.2  29.0  24.3  18.1   8.6   0.9
Observed monthly ave min temperature (C)
-11.5  -8.6  -2.8   4.3  10.9  16.2  18.9  17.6  12.3   5.9  -1.6  -8.2
Observed monthly ave solar radiation (Langleys/day)
176.0 255.0 328.0 405.0 482.0 542.0 538.0 462.0 369.0 276.0 189.0 145.0
Observed monthly ave precipitation (mm)
 34.2  39.5  69.8  90.3 112.5 121.2 113.8 119.7  97.6  80.7  65.5  41.6
```

Figure 4.1: Wepp climate file header section

The header section of the climate file characterizes the location where the rain fall gauge resides with parameters like latitude and longitude, characterizes the on site climate conditions with averaged parameters (minimum and maximum monthly temperature, solar radiation and precipitation) and finally defines some flags for the WEPP simulation. Detailed information on the individual parameter can be found in Flanagan and Livingston (1995).

The body of the climate file holds the values for the following parameters (Flanagan and Livingston, 1995) excluding the rainfall related parameters for the moment because these parameters vary between the two different layout types.

Table 4.1: Parameters included in the body of the climate file

Parameter Abbreviation	Parameter Meaning	Unit
da/mo/year	day/month/year	
tmax	daily maximum temperature	(C°)
tmin	daily minimum temperature	(C°)
rad	daily solar radiation	(langleys/day)
w-vl	wind velocity	(m/sec)
w-dir	wind direction	(degrees from North)
tdew	dew point temperature	(C°)

4.1.1 Rainfall related parameters

A basic layout of rainfall measurement data follows the layout presented in Table 4.2.

Table 4.2: Basic data layout recorded by a rain gauge

Data	Time	Amount of Precipitation (mm)	Temperature (C°)
24.02.2003	00:00	0.0	20.4
24.02.2003	00:05	0.0	20.1
24.02.2003	00:10	0.0	19.3
24.02.2003	00:15	0.0	19.9
24.02.2003	00:20	0.0	20
24.02.2003	00:25	0.1	19.1
24.02.2003	00:30	0.1	20.5

The focus on theses data in terms of erosion is not so much on the total amount of rainfall within a certain period of time. The focus is on the rain storm intensity and the storm energy. So the rainfall data needs to be disaggregated and transformed into a WEPP readable layout.

No-Breakpoint-Layout

Figure 4.2 exemplifies the no-breakpoint-layout.

```
da mo year  prcp   dur    tp     ip    tmax  tmin rad  w-vl w-dir tdew
             (mm)   (h)                 (C)   (C) (l/d)(m/s) (Deg)  (C)
 1  1    1   4.5  1.21  0.02   1.01   -4.8 -12.5  76.   6.8 312.  -8.7
 2  1    1   0.0  0.00  0.00   0.00 -10.2 -16.9 136.   6.9 301. -13.5
```

Figure 4.2: No-breakpoint layout

The previously skipped (Table 4.1) rainfall related parameters are presented next.

Table 4.3: Rainfall related parameters included in the body of the climate file

Parameter Abbreviation	Parameter Meaning	Unit
prcp	Precipitation	(mm)
dur	Duration	(h)
tp	Normalized time to peak	
ip	Normalized peak intensity	

Precipitation summarizes the total amount of rainfall of one storm and duration holds the total time of the storm. The normalized time to peak is calculated by the time to the maximum intensity of the storm divided by the total storm duration.

$$t_p = \frac{D_p}{D} \qquad [10]$$

The normalized peak intensity is calculated by maximum intensity of the storm divided by the average intensity of the storm.

$$i_p = \frac{r_p}{i_b} \qquad [11]$$

Breakpoint layout

Figure 4.3 exemplifies the no-breakpoint-layout.

```
 da mo year  nbkpt tmax  tmin rad  w-vl w-dir tdew
             (#)   (C)   (C) (l/d)(m/s) (Deg)  (C)
 23  3   94  27    8.3  -2.3 145.  6.7 306.   2.8
17.03 0.00
17.12 0.508
17.75 0.508
```

Figure 4.3: Breakpoint layout

Breakpoint layout uses two columns to characterize the storm. One column holds the accumulated time of each storm and the other holds the accumulated precipitation of each storm. Additionally the parameter “nbkpt” is defined which holds the number of breakpoints for each storm event. The maximum value of this parameter is limited to 50 in current versions of the WEPP model.

4.2 Soil input parameters

Based on the fact that WEPP is categorized as a processed base model the model's demand on input parameters is high. Figure 4.4 summarizes the required input parameters regarding the soil properties. There are basically three sections of parameters. Firstly some description of the actual input file represented by "Soil File Name" and "Soil Texture", secondly six parameters including the baseline erodibility parameters, the soil Albedo, the initial soil saturation level and the effective hydraulic conductivity and thirdly the textural description of the existing soil layers on a vertical view. The origin of the vertical axis resides at soil surface.[2]

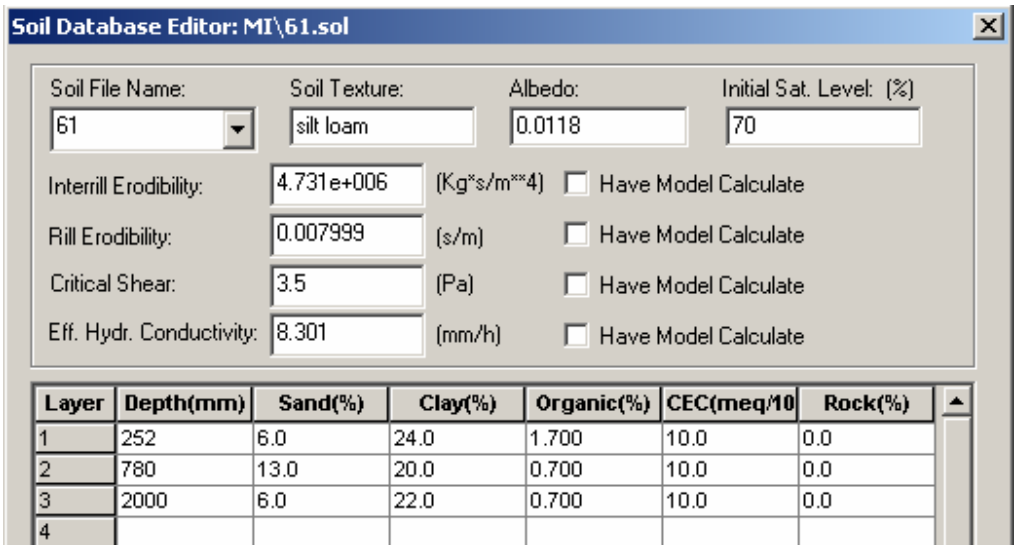

Figure 4.4: Soil parameter input mask (WEPP, 1995)

4.2.1 Baseline soil erodibility parameter estimation

WEPP is very sensitive to baseline interrill erodibility input as there are interrill erodibility (K_i), rill erodibility (K_r) and critical hydraulic shear (τ_c). The outlined equation delivers a value for the specific parameter regarding freshly tilled soil with no residue present (Flanagan and Livingston, 1995).

Cropland: soils containing $\geq$ 30% sand:

$$K_i = 2272800 + 192100 \cdot VFS \qquad [12]$$

where:

[2] The outlined equations can be found in Flanagan and Livingston (1995)

K_i = interrill erodibility

VFS = very fine sand

$$K_r = 0.00197 + 0.00030 \cdot VFS + 0.03863 \cdot EXP(-1.84 \cdot ORGMAT) \quad [13]$$

where:

K_r = rill erodibility

VFS = very fine sand

$ORGMAT$ = percent organic matter in surface soil (about 1.724 times organic carbon content)

$$\tau_c = 2.67 + 0.065 \cdot CLAY - 0.058 \cdot VFS \quad [14]$$

where:

τ_c = critical hydraulic shear

$CLAY$ = percent clay

VFS = very fine sand

The assumptions incorporated by these equations are as follows:

VFS $\leq$ 40% if value is greater than 40%, use 40%
ORGMAT $\geq$ 35% if value less than 35%, use 35%
CLAY $\leq$ 40% if value greater than 40%, use 40%

Cropland: soils containing $\leq$ 30% sand:

$$K_i = 6054000 - 55130 \cdot CLAY \quad [15]$$

where:

K_i = interrill erodibility

$CLAY$ = percent clay

$$K_r = 0.0069 + 0.134 \cdot EXP(-0.20 \cdot CLAY) \quad [16]$$

where:

K_r = rill erodibility

$CLAY$ = percent clay

$$\tau_c = 3.5 \quad [17]$$

where:

τ_c = critical hydraulic shear

There is again one assumption included, namely clay content must be $\geq$ 10%. If value is less than 10%, 10% should be used.

4.2.2 Soil Albedo

Soil Albedo stands for the fraction of the solar radiation which is reflected back into the atmosphere after soil surface contact. The following equation can be used to calculate an estimate for the soil Albedo assuming a dry surface.

$$SALB = \frac{0.6}{e^{(0.4 \cdot ORGMAT)}} \quad [18]$$

where:

$ORGMAT$ = percent organic matter in surface soil

4.2.3 Initial Saturation

$$\left(SOILWA, m/layer\right) = \left(SAT \cdot POR \cdot RFG\right) \cdot DG \quad [19]$$

where:

POR = layer's porosity $\frac{cm^3}{cm^3} = \frac{1-bd}{2.65}$

RFG = correction of porosity for rock content

DG = thickness of soil layer (m)

4.2.4 Effective Conductivity Estimation

Soils with $\leq$ 40% clay

$$K_b = -0.265 + 0.0086 \cdot SAND^{1.8} + 11.46 \cdot CEC^{-0.75} \quad [20]$$

where:

$SAND$ = percent of sand

CEC = cation exchange capacity (meq/100g)

Soils with ≥ 40% clay

$$K_b = 0.0066 \cdot e^{\frac{244}{CLAY}} \quad [21]$$

where: $CLAY$ = percent of clay

4.2.5 Soil related parameterization of Mistelbach watershed

The soil related parameterization of Mistelbach watershed is summarized next (Table 4.5). The initial saturation level is assumed with 70% and refers to the 1st January of first simulation. All other parameters contained by Table 4.4 are derived by the usage of the previously described equations.

Table 4.4: First parameter set of soil input file

Soil definition	13	14	33	50	61	9
Albedo	0.0134	0.0177	0.0134	0.0105	0.0118	0.0163
Initial Sat. Level (%)	70	70	70	70	70	70
Interrill erodibility (kg/sm4)	5.01E+06	4.79E+06	4.29E+06	4.95E+06	4.73E+06	4.73E+06
Rill erodibility (s/m)	0.009902	0.008199	0.0071	0.0094	0.007999	0.007999
Critical shear (Pa)	3.5	3.5	3.5	3.5	3.5	3.5
Eff. hydr. Conductivity (mm/h)	8.301	8.301	8.301	1.3	8.301	26.29

The input values of Table 4.5 are derived by the analysis of sieving curves. Additional chemical analysis must be executed in order to derive values for organic material content and cation exchange capacity (CEC).

Table 4.5: Second parameter set of soil input file

Layer	Soil definition	Depth (mm)	Sand (%)	Clay (%)	Org. material (%)	CEC (meq/100g)	Rock (%)
	13	300	15	19	2	10	0
	14	300	10	23	2.7	10	0
	33	250	10	32	2	10	0
	50	252	9	20	1.4	10	0
1	61	252	6	24	1.7	10	0
	9	250	22	24	2.5	10	0
	13	400	12	20	1.5	10	0
	14	500	9	24	2	10	0
	33	550	8	35	0.9	10	0
	50	780	10	18	0.2	10	0
2	61	780	13	20	0.7	10	0
	13	900	11	15	0.6	10	0
	14	600	8	23	1.3	10	0
	33	900	9	19	0.3	10	0
	61	2000	6	22	0.7	10	0
3	9	900	21	24	1.9	10	0
4	14	900	10	17	0.7	10	0

4.3 Management file

The management input file comprehensively summarizes parameters (Figure 4.5) related to management practices applied to arable land and related to crops either planted during the current growing season or harvested the prior year.

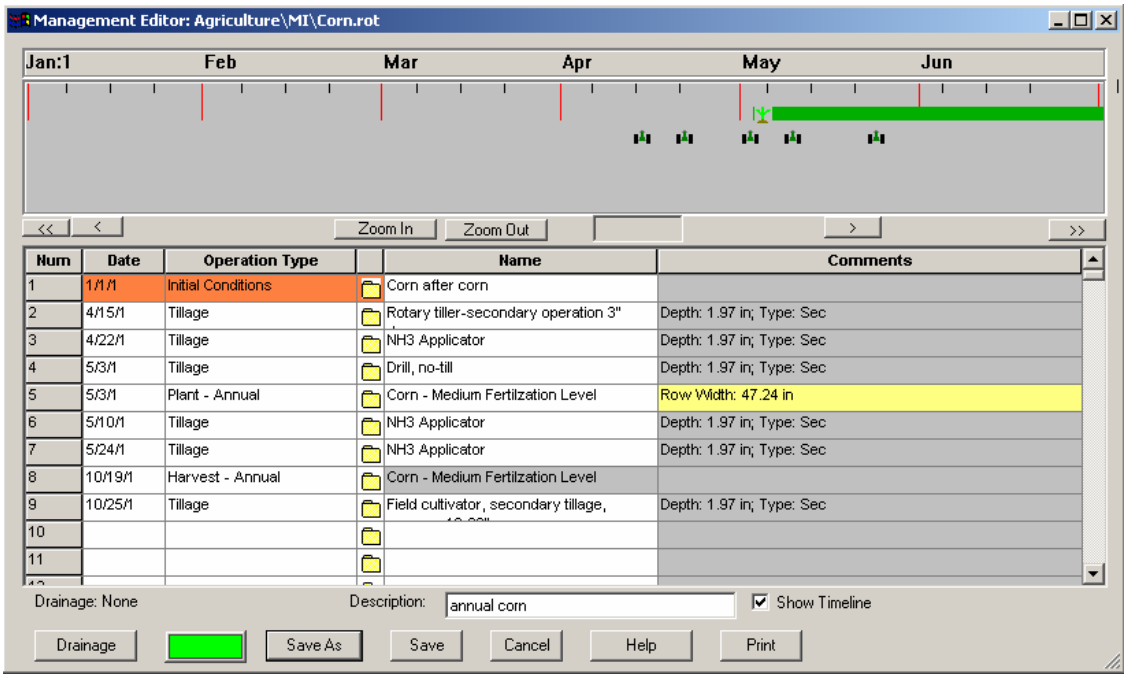

Figure 4.5: Management definition

The definition of the parameters follows the schema: which operation, defined by the operation type is applied when and adds what subset of parameters to the model. Depending on the operation type a specific subset of available parameters is offered by the model. The definition of Mistelbach watershed management deals with three operation types namely “initial conditions”, “tillage” and “plant/harvest”.

4.3.1 Initial conditions

This operation type defines the in situ conditions on 1st January of the actual simulation year. This means within this operation type the model can be adapted to perennial cropping cycles as well as annual cropping cycles where the planted crop was harvested in the fall one year prior.

Table 4.6: Initial conditions - parameter set

Parametername	
Initial Plant	Initial roughness after last tillage
Bulk density after last tillage	Rill spacing
Initial canopy cover (0-100%)	Rill width type
Days since last tillage	Initial snow depth
Days since last harvest	Initial depth of thaw
Initial frost depth	Depth of secondary tillage layer
Initial interrill cover (0-100%)	Depth of primary tillage layer
Initial residue cropping system	Initial rill width
Cumulative rainfall since last tillage	Initial total dead root mass
Initial ridge height after last tillage	Initial total submerged residue mass
Initial rill cover (0-100%)	

4.3.2 Tillage

This operation type holds all parameters linked to any management operation applied to the arable field including plowing, harrowing, field cultivation, planting, harvesting, fertilization and herbicide application. A principal differentiation of the applied operation type is made by the separation into primary and secondary tillage operation which refers to depth of soil which is disturbed by the specific operation type.

Table 4.7: Tillage operation - parameter set

Parametername
Percent residue buried on interrill areas for fragile crops
Percent residue buried on interrill areas for non-fragile crops
Number of rows of tillage implement
Implement Code
Cultivator Position
Ridge height value after tillage
Ridge interval
Percent residue buried on rill areas for fragile crops
Percent residue buried on rill areas for non-fragile crops
Random roughness value after tillage
Surface area disturbed (0-100%)
Mean tillage depth

4.3.3 Planting

This operation type adds parameters linked to the planted crop and is categorized by the six following categories:

- plant growth and harvest parameters
- temperature and radiation parameters
- canopy, LAI and root parameters
- senescence parameters
- residue parameters
- other parameters

4.3.4 Management parameterization for Mistelbach watershed

For obvious reasons it is not possible to go too much into detail on the management parameterization of Mistelbach watershed. Therefore a summarization of applied management practices and planted corps is presented by the following tables categorized by annual and perennial crops.

Table 4.8: Annual crops

Operation Type	Operation Name	Corn	Peas	Summer Barley
Initial condition	After Barley with Fall Chisel			
Tillage	Rotary tiller-secondary operation 3" deep	15.04.2003	15.03.2003	15.03.2003
Fertilizer application	NH3 Applicator	22.04.2003	22.03.2003	22.03.2003
Planting	Drill, no-till	03.05.2003	06.04.2003	06.04.2003
Fertilizer application	NH3 Applicator	10.05.2003	16.04.2003	16.04.2003
Herbicide application	NH3 Applicator	24.05.2003	27.04.2003	27.04.2003
Harvest	NH3 Applicator	19.10.2003	15.08.2003	12.08.2003
Tillage	Field cultivator, secondary tillage, sweeps 12-20"	25.10.2003	22.08.2003	18.08.2003

Table 4.9: Perennial crops

Operation Type	Operation Name	Canola	Winter wheat
Initial condition	Customized Continuous alfalfa initial conditions		
Harvest	NH3 Applicator	15.08.2003	05.08.2003
Tillage	Field cultivator, secondary tillage, sweeps 12-20"	21.08.2003	21.08.2003

Operation Type	Operation Name	Forest	Gras
Initial condition		Tree-20 yr forest	grass strip

Chapter 5

Resampling Strategy

5.1 Search Strategy[3]

The search neighborhood defines the sample data which are actually included in the local estimation procedure based on the definition of the search geometry. This definition is based on the investigation on spatial continuity pattern of the sample data. Usually the point where the estimation procedure is applied builds the center of the search geometry. Depending on the revealed spatial continuity pattern of the sample data anisotropy can also be taken into consideration, firstly by the shape of the search geometry and secondly by the ratio of anisotropy. This means that the spatial continuity is more obvious in one direction than into any other and finally that the estimation value at the point of interest is not solemnly dependent on the magnitude of separation of considered sample data, but also on the direction where the sample data resides.

The necessity of selecting a specific set of sample data is only apparent when the estimation procedure can accommodate various sample data for local estimation, like inverse distance weight or ordinary kriging methods. While defining the search neighborhood Isaaks and Srivastava (1989) proclaim the following questions to be seriously considered.

- are there enough nearby samples?
- are there too many samples?
- are there nearby samples that are redundant?
- are the nearby samples relevant?

As some verifiable definitions for the first three questions exist there are many assumptions included in the last question dependent on the study's goals and subjective definitions. Therefore a reformulation of the originally asked question (Do the considered sample data belong to the same group as the point estimated?) may narrow the amount of suitable answers.

Answering the first question defines the minimum size of search geometry based on definition of a minimum number of sample data necessary to consider with the estimation procedure. The minimum number is strongly related to sample data's geometry. In case of (pseudo) regularly

[3] see Isaaks and Srivastava (1986), Chapter 14

gridded data a minimum of four, practically a minimum of 12 samples can be taken as a guideline. Dealing with irregularly gridded data, the minimum size of search geometry can be crudely calculated from the formula:

$$average\,spacing\,between\,data \approx \sqrt{\frac{Total\,area\,\mathrm{cov}ered\,by\,samples}{Number\,of\,samples}} \qquad [22]$$

The second question tries to answer how much bigger than the minimum size the search geometry should be. There are two facts to be considered, firstly the computational time and secondly the discrepancy between theoretical statistical properties predicted by the used model and observed statistics of the sample data. The conceptualization of sample data with a stationary random function model includes theoretically an improvement of the estimate as the amount of considered sample data increase. Stationarity considers the relation of any sample point to the estimate dependent on the separation distance and in case of anisotropy of direction. This assumption does not necessarily need to meet reality, as farther samples may not have any relation with the estimate. Hence the reduction of considered sample points is achieved by the application of a search geometry which is also narrowing the gap between reality and theory.

Consideration of computational time also plays a role by the definition of the search geometry. Thinking of calculating ordinary kriging weights a doubling of sample data results in an eightfold of calculations necessary because the computation requirement increases by the cube of considered samples. Again a reasonable consideration of sample points can help.

And finally the question of redundancy can be addressed by applying a search geometry including the possibility for a quadrant search. Although ordinary kriging involves a consideration of redundant sample data in the conceptualization of the method itself (C-Matrix) it is believed that the quadrant search improves the estimates derived. Within each quadrant the maximum and minimum number of sample data evaluated by the applied estimation method is defined. In case that the amount of actual sample data exceeds maximum number only the closest sample data is considered.

The parameterization for inverse distance weight and ordinary kriging resampling strategy used for this study is presented in Figure 5.1. Due to the fact that the location of sample values was evenly spaced and that elevation showed a continuous behavior the proposed values were taken for the resampling procedure.

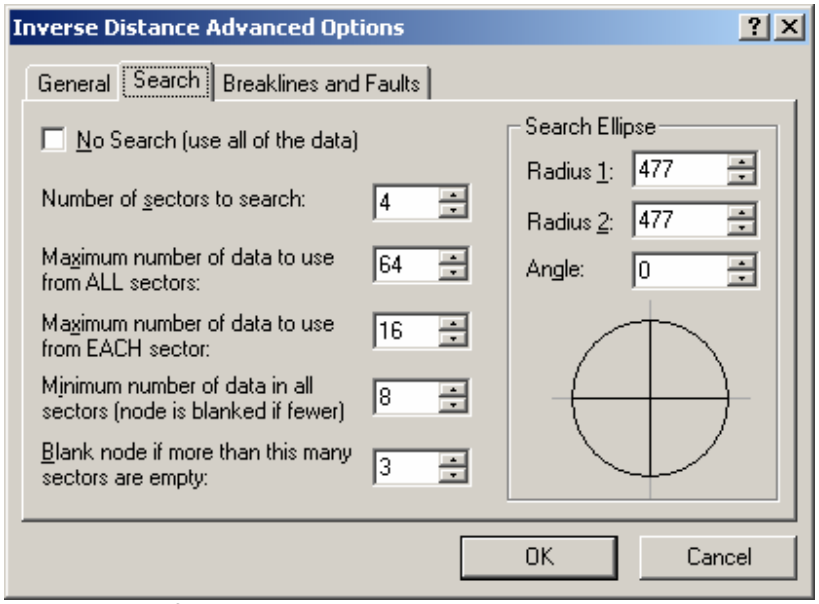

Figure 5.1: Search parameterization for inverse distance weight and ordinary kriging method

5.2 Resampling Strategies

The resampling in this study was achieved by the application of algorithms implemented in SURFER 8.02 software (Golden Software, 2002). Some basic principles of strategies applied within this study are discussed in the following section.

5.2.1 Nearest Neighborhood

Since the methodology incorporated into nearest neighbor resampling strategy is rather simple, only a brief description is given. Nearest neighbor method (Golden Software, 2002) assigns that sample value to estimate that is closest to location of estimate according to the spatial pattern of the sample values. One important aspect about this assignment is that the search radius must be large enough that the algorithm can find a location and a corresponding sample value. If this condition cannot be met the estimate is assigned a “no value”.

In present study the search radius included the total area thus at each estimate location a sample value was assigned.

5.2.2 Inverse Distance Methods

This estimation method builds on a weighted linear combination as follows (Isaaks and Srivastava, 1989):

$$estimate = \hat{v} = \sum_{i=1}^{n} w_i \cdot v_i \qquad [23]$$

where:

$v_1, v_2, ..., v_n$ sample data used for estimation

$w_1, w_2, ..., w_n$ assigned weight to the corresponding sample data

In case of inverse distance weight methods, the magnitude of the assigned weight decreases as the distance of the sample point increases to the location of the point estimated. The sum of all assigned weights considered by the estimation procedure equals to one based on the unbiasedness condition. This leads to the following formulation (Isaaks and Srivastava – chapter 11, 1989):

$$\hat{v}_i = \frac{\sum_{i=1}^{n} \frac{1}{d_i^p} v_i}{\sum_{i=1}^{n} \frac{1}{d_i^p}} \qquad [24]$$

where:

$v_1, v_2, ..., v_n$ sample data used for estimation

$\frac{1}{d_i^p}$ weight inversely proportional to any power of the distance

5.2.3 Ordinary Kriging[4]

This estimation method is again a weighted linear combination. A comprehensive explanation of this method cannot be given based on the fact that this exceeds the scope of this work. In spite a brief summary should provide an overview of the concept.

Given a set of sample data the first step in the cycle of ordinary kriging application is the description of the spatial continuity pattern of the sample data by the means of correlogram, covariance or the variogram. In case that spatial continuity is solemnly dependent on separation of sample data anisotropy need not be considered. In case that spatial continuity is more obvious in one direction than in another direction, anisotropy needs to be taken into account.

The weighted linear combination for the estimate is as following:

$$\hat{v} = \sum_{i=1}^{n} w_i \cdot v_i \qquad [25]$$

where:

[4] see Isaaks and Srivastava (1986), Chapter 12

$v_1, v_2, ..., v_n$ sample data used for estimation

$w_1, w_2, ..., w_n$ assigned weight to the corresponding sample data

The residual is defined as follows:

$$Error\ of\ i^{-th}\ estimate = r_i = \hat{v}_i - v_i \quad [26]$$

where:

$\hat{v}_i$ estimate at location i

v_i true value at location i

Like the inverse distance weight methods, ordinary kriging aims unbiasedness ($\tilde{m}_R$ = 0) and additionally the minimization of the error variance ($\tilde{\sigma}_R^2$ = min) which is practically unattainable because access to the exhaustive dataset which could provide an accessible distribution of the parameter of interest as well as a deterministic description of parameter's behavior are not available in almost any case. The resulting difficulty can be shown as following:

$$m_R = \frac{1}{k}\sum_{i=1}^{k} \hat{v}_i - v_i \quad [27]$$

where:

m_R average error

k number of estimates

$\hat{v}_i - v_i$ difference of estimated value and true value

Per se the method tries to calculate the average error by sticking to the unbiasedness condition. This attempt aims to reduce the average error to zero by facing the actual shortcoming of unknown true values (v_i). The conceptualization of this dead end is that the estimates as well as the true values are seen as random variables that are governed by a stationary random function model and that every value in this model is seen as the outcome of random variables. The estimation of unknown value incorporating the random model approach follows the expression:

$$\hat{V}(x_o) = \sum_{i=1}^{n} w_i \cdot V(x_i) \qquad [28]$$

Where:

$\hat{V}(x_o)$	estimated random variable at point of interest
w_i	weight
$V(x_i)$	sample data conceptualized as outcome of stationary random function model

The previously presented equation is after a considerable amount of math finally converted into the so called ordinary kriging system which is given by the following equation.

$$w = C^{-1} \cdot D \qquad [29]$$

where:

w	weight matrix
C	covariance matrix of any pair of points
D	covariance matrix of any point and point of estimation

All covariances necessary for the computation of the estimates are derived from the model function. The appropriateness of the chosen model shows significant influence on the quality of estimation based on the conceptualization of the ordinary kriging method. One strong recommendation therefore is that the random function model reflects the spatial continuity pattern of the available sample data.

The four model properties that are finally discussed are scale, shape, nugget effect and range (Isaaks and Srivastava, 1989). The model's scale does not show any influence on ordinary kriging weights nor estimates but effects the ordinary kriging variance. The shape steers the assigned influence of surrounding sample data on the estimate. A parabolic model behavior near the origin indicates a very continuous phenomenon. The nugget effect accounts for discontinuities at very short distances. Given the consideration of a nugget effect the calculated weights are more similar than without consideration. The definition of the range shows minor effects on the weights but noticeable influence on estimates. Given all these possibilities for model adjustment once more the recommendation of an appropriately spatial continuity pattern modeling of the sample data is inevitable for the successful application of the ordinary kriging methodology.

After all this theory that yields to estimates derived by ordinary kriging the parameterization of this method used in this study is presented next. Sample values were described omnidirectionally with the experimental variogram indicating a strong continuity reflected by the parabolic behavior at variogram origin. This behavior is accounted for with a Gaussian variogram model that was fitted to reflect this observation by calculated estimates.

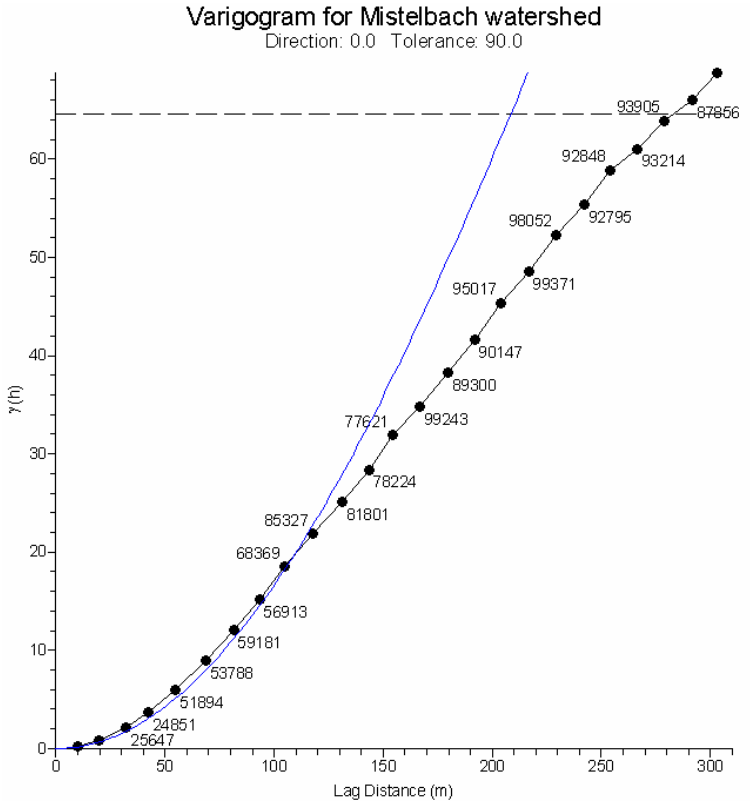

Figure 5.2: Variogram for Mistelbach watershed

5.3 Analysis of resampling strategies

Applying resampling strategies leads to a new set of the native sample dataset. In case of this study the sample dataset is built by a DEM of 10m spatial resolution. This dataset is seen as the best representation of reality available and therefore referred to as the true value. At this point it is clearly stated that this approach includes the assumption that given the actual possibilities of the representation of the study area's landscape this approach can be justified knowing about possible shortcomings.

Incorporating this DEM into the resampling strategy means that a regular grid of 10m distance in each direction of a sample point is available throughout the whole area of investigation. This dataset builds the basis for resampling. The goal of applied resampling is twosome: Firstly an increase of native spatial resolution of 10m to 7.5m, 5m and 2.5m and secondly a decrease of native spatial resolution to 15m and 20m. Regarding three different resampling strategies and 5 aimed spatial resolutions this approach yields 15 resampled digital elevation models.

As mentioned the application of resampling strategies leads to a new set of the original data. Aim of any resampling strategy is to represent the original dataset as comprehensively and precisely as possible. Reality regularly shows that there is a discrepancy between theory and praxis included with the application of any resampling procedure leading to the necessity of means to quantify this discrepancy in order to make an assessment on the usability of the resampling strategy for a specific purpose.

In this study means of descriptive statistics are used to compare the statistics of true values distribution to statistics of estimated values distribution. Secondly statistics on calculated residuals is executed to give some understanding of the influence of the specific resampling strategy on the quality of the estimates. The following tables compare the statistics on true values (native 10m) to the estimated values of any resolution investigated sorted by the applied resampling strategy.

Table 5.1: Comparison of true and estimated values (m) using inverse distance weight method

Spatial Resolution	20m	15m	7.5m	5m	2.5m	Native 10m
Number of values	585	1039	4145	9337	37339	2332
Mean	251.941	251.947	251.971	251.977	251.975	251.980
Standard deviation	7.967	7.991	7.975	7.982	7.981	8.040
Variance	63.471	63.864	63.598	63.707	63.689	64.628
Coefficient of variation	0.032	0.032	0.032	0.032	0.032	0.032
Minimum	232.123	232.006	231.730	231.653	231.575	231.562
First quartile	246.612	246.721	246.625	246.658	246.663	246.662
Median	252.972	253.045	253.131	253.122	253.124	253.138
Third quartile	258.437	258.497	258.553	258.555	258.555	258.597
Maximum	264.627	264.829	264.896	264.927	264.964	264.972
Range	32.504	32.823	33.167	33.275	33.389	33.41
Coefficient of correlation	0.999	0.999	1	1	1	

Table 5.2: Comparison of true and estimated values (m) using nearest neighbor method

Spatial Resolution	20m	15m	7.5m	5m	2.5m	Native 10m
Number of values	585	1039	4145	9337	37337	2332
Mean	251.883	251.959	251.948	251.985	251.949	251.980
Standard deviation	8.047	8.045	8.026	8.036	8.034	8.039
Variance	64.754	64.721	64.421	64.577	64.553	64.628
Coefficient of variation	0.032	0.032	0.032	0.032	0.032	0.032
Minimum	231.562	231.835	231.562	231.562	231.562	231.562
First quartile	246.542	246.739	246.652	246.666	246.590	246.662
Median	252.944	253.129	253.138	253.157	253.138	253.138
Third quartile	258.486	258.597	258.574	258.597	258.564	258.597
Maximum	264.899	264.905	264.972	264.972	264.972	264.972
Range	33.337	33.070	33.410	33.410	33.410	33.410
Coefficient of correlation	0.99778	0.99935	0.99959	1	1	

Table 5.3: Comparison of true and estimated values (m) using ordinary kriging method

Spatial Resolution	20m	15m	7.5m	5m	2.5m	Native 10m
Number of values	585	1039	4145	9337	37339	2332
Mean	251.926	251.946	251.966	251.971	251.967	251.980
Standard deviation	8.049	8.043	8.026	8.034	8.034	8.039
Variance	64.791	64.696	64.416	64.542	64.543	64.628
Coefficient of variation	0.032	0.032	0.032	0.032	0.032	0.032
Minimum	231.678	231.710	231.605	231.601	231.530	231.562
First quartile	246.735	246.664	246.626	246.633	246.629	246.662
Median	253.056	253.074	253.141	253.155	253.140	253.138
Third quartile	258.484	258.509	258.550	258.548	258.549	258.597
Maximum	264.875	264.882	264.993	265.007	265.006	264.972
Range	33.197	33.172	33.388	33.406	33.475	33.41
Coefficient of correlation	1	1	1	1	1	

Regarding the residuals Isaaks and Srivastava (1986) argue that the distribution of estimates should reflect the same statistical characteristics as the distribution of the true values. The statistical parameters mean, median and standard deviation were calculated by using resampling results derived by different resampling strategy at all spatial resolutions of interest. The observation that parameters derived from resampled data and those derived from native data fall very close to each other can be made. Actual differences of only a few centimeters can be identified. Coefficient of correlation also shows high accordance of estimated and true values. Remarkable are the minimum and maximum estimation values of ordinary kriging. As mentioned this method can estimate maximum and minimum values larger respectively smaller than the maximum and minimum values of the sample dataset which is the case at 2.5m resolution (Table 5.3).

The calculation of residuals in combination with the calculation of statistics on the residuals provides a different view on the estimated values.

$$error = r = \hat{v} - v \qquad [30]$$

where:

$\hat{v}$ … estimated value

v … true value

The following two tables provide calculated statistical values firstly for decrease spatial resolution and secondly for increased spatial resolution.

Table 5.4: Statistics on residuals (m) of decreased spatial resolution

Spatial Resolution		**20m**			**15m**	
Resampling Strategy	**IDW**	**NN**	**OK**	**IDW**	**NN**	**OK**
Number of values	2193	2193	2193	2231	2231	2231
Mean	-0.030	0.041	-0.007	-0.012	-0.017	-0.003
Standard deviation	0.253	0.378	0.095	0.208	0.204	0.067
Variance	0.064	0.143	0.009	0.043	0.042	0.005
Coefficient of variation	-8.460	9.200	-14.121	-17.031	-11.698	-19.398
Minimum	-0.998	-1.189	-0.611	-0.684	-0.629	-0.486
First quartile	-0.112	-0.135	-0.025	-0.091	-0.129	-0.018
Median	-0.010	0.093	0.003	-0.009	-0.029	0.002
Third quartile	0.067	0.255	0.028	0.047	0.071	0.021
Maximum	1.659	0.948	0.424	1.894	0.832	0.287
Range	2.657	2.137	1.035	2.578	1.461	0.773
Mean Absolute Error	0.163	0.295	0.056	0.131	0.149	0.040
Mean Squared Error	0.065	0.144	0.009	0.043	0.042	0.005

At first glance the values of calculated means of the two weighted linear combination methods (IDW and OK) are very close to zero which reflects one aim of these methods (unbiasedness condition). Additionally OK tries to minimize the variance which is also reflected by the values of Table 5.4. A negative mean leads to the assumption that the methods tend to underestimate true vales which is the case in actual dataset except for 20m spatial resolution derived by nearest neighbor method.

This assumption is also supported by the existing median of residual values that is again very close to zero. Regarding mean absolute error (MAE) and mean squared error (MSE) (Isaaks and Srivastava, 1986)

$$MAE = \frac{1}{n}\sum_{i=1}^{n}|r| \quad [31]$$

$$MSE = \frac{1}{n}\sum_{i=1}^{n}r^2 \quad [32]$$

ordinary kriging succeeds over all other methods showing definitely the smallest values for both parameters.

Regarding the increased spatial resolution of the DEM derived by the application of the same resampling strategies it becomes obvious that nearest neighbor method reproduces the true values exactly for 5m and 2.5m resolution. Normally this situation would be desired but considering how the estimates are derived by nearest neighbor methods the conclusion of an unrealistic and unwanted reproduction has to be drawn. Again mean and median values are very close to zero while with an increase of spatial resolution the negativity of mean decreases. In other words the underestimation of estimates decreases. Standard deviation and variance also decrease with an increase in spatial resolution.

Table 5.5: Statistics on residuals (m) of increased spatial resolution

Spatial Resolution	**7.5m**			**5m**			**2.5m**		
Resampling Strategy	**IDW**	**NN**	**OK**	**IDW**	**NN**	**OK**	**IDW**	**NN**	**OK**
Number of values	2276	2276	2276	2298	2298	2298	2301	2301	2301
Mean	-0.011	0.014	-0.001	0.001	0	0.000	-0.003	0	0.000
Standard deviation	0.181	0.161	0.046	0.101	0	0.049	0.043	0	0.038
Variance	0.033	0.026	0.002	0.010	0	0.002	0.002	0	0.001
Coefficient of variation	-16.046	11.379	-49.771	202.027	33.890	-115.710	-13.819	n.a.	-86.868
Minimum	-0.752	-0.855	-0.423	-1.034	0	-0.412	-0.240	0	-0.332
First quartile	-0.083	-0.032	-0.014	-0.030	0	-0.015	-0.025	0	-0.013
Median	-0.012	0.000	0.001	0.004	0	0.000	-0.005	0	0.000
Third quartile	0.044	0.082	0.014	0.030	0	0.014	0.011	0	0.011
Maximum	1.130	0.627	0.359	2.244	0	0.352	0.456	0	0.323
Range	1.881	1.482	0.783	3.278	0	0.764	0.696	0	0.656
Mean Absolute Error	0.118	0.101	0.027	0.057	0	0.029	0.030	0	0.022
Mean Squared Error	0.033	0.026	0.002	0.010	0	0.002	0.002	0	0.001

So far the provided statistics dealt with the statistics of either the distribution of estimated values or the distribution of residuals. Table 5.4 and Table 5.5 provided some evidence that the criterion of global unbiasedness is met fairly well. On the other hand global unbiasedness does not necessarily provide conditional unbiasedness. Conditional unbiasedness means that the bias for a group of values taken from the distribution equals zero. Observing that all investigated groups show unbiasedness means that the condition of global unbiasedness is met. The upcoming graphs show

scatter plots where estimated values are plotted against residuals. This representation reveals that the conditional unbiasedness in the investigated context is strongly dependent on the applied method. Regarding ordinary kriging conditional unbiasedness can be found in case of increase spatial resolution while on the other hand in case of decrease conditional unbiasedness can partially be found. Inverse distance weight partially meets conditional unbiasedness at very high spatial resolution while nearest neighbor hardly meets conditional unbiasedness.

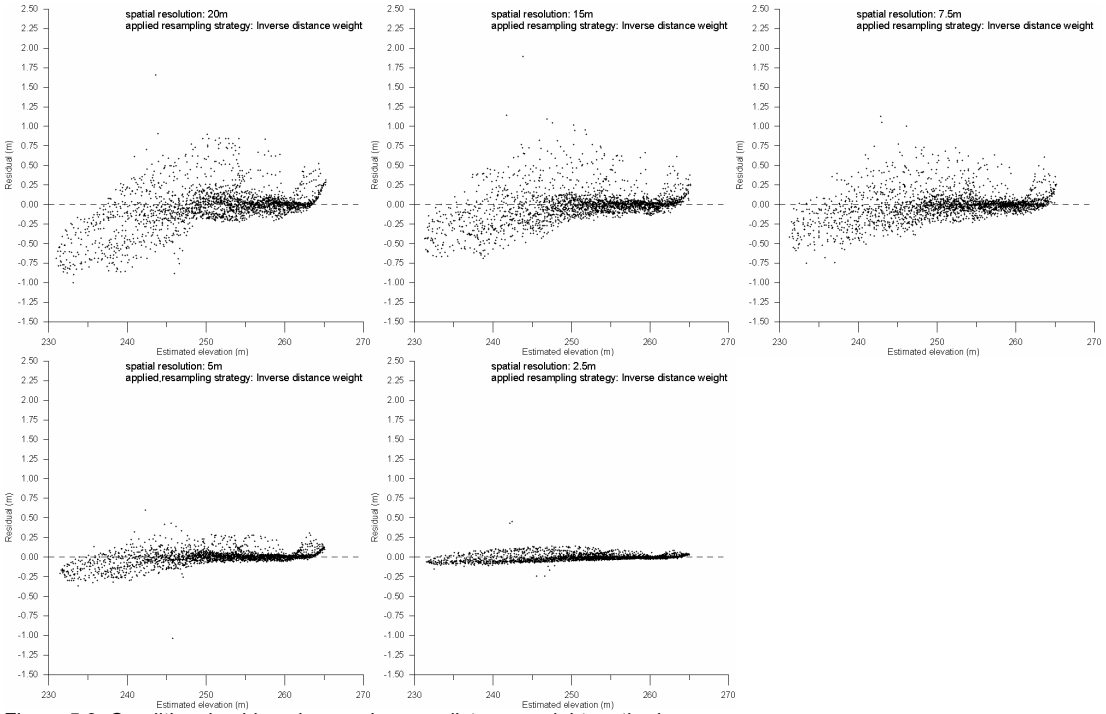

Figure 5.3: Conditional unbiasedness – Inverse distance weight method

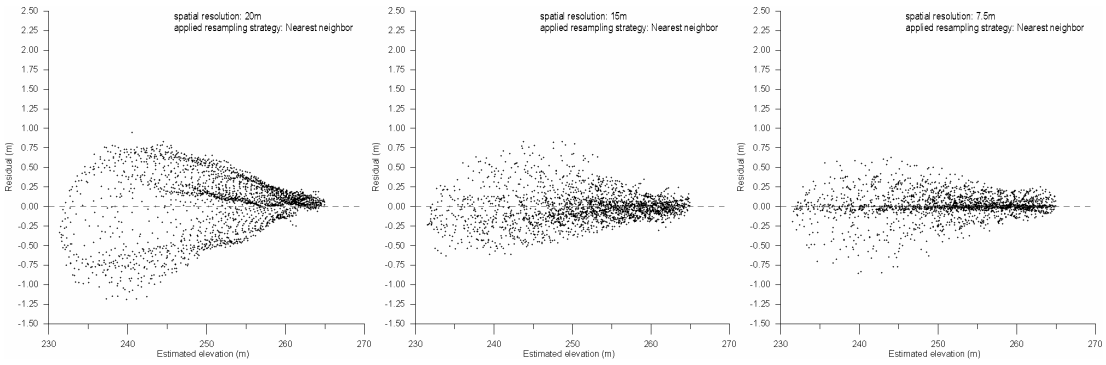

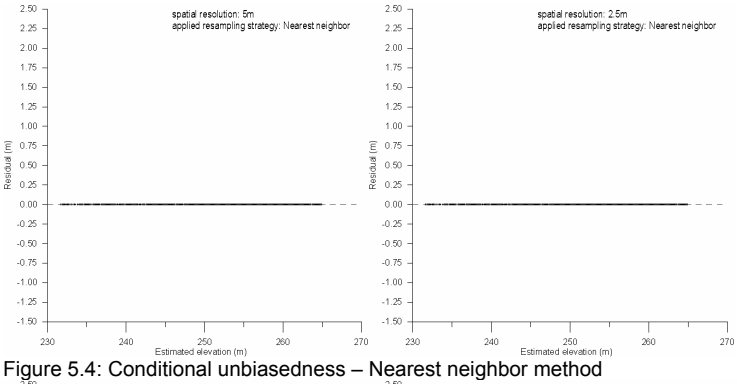

Figure 5.4: Conditional unbiasedness – Nearest neighbor method

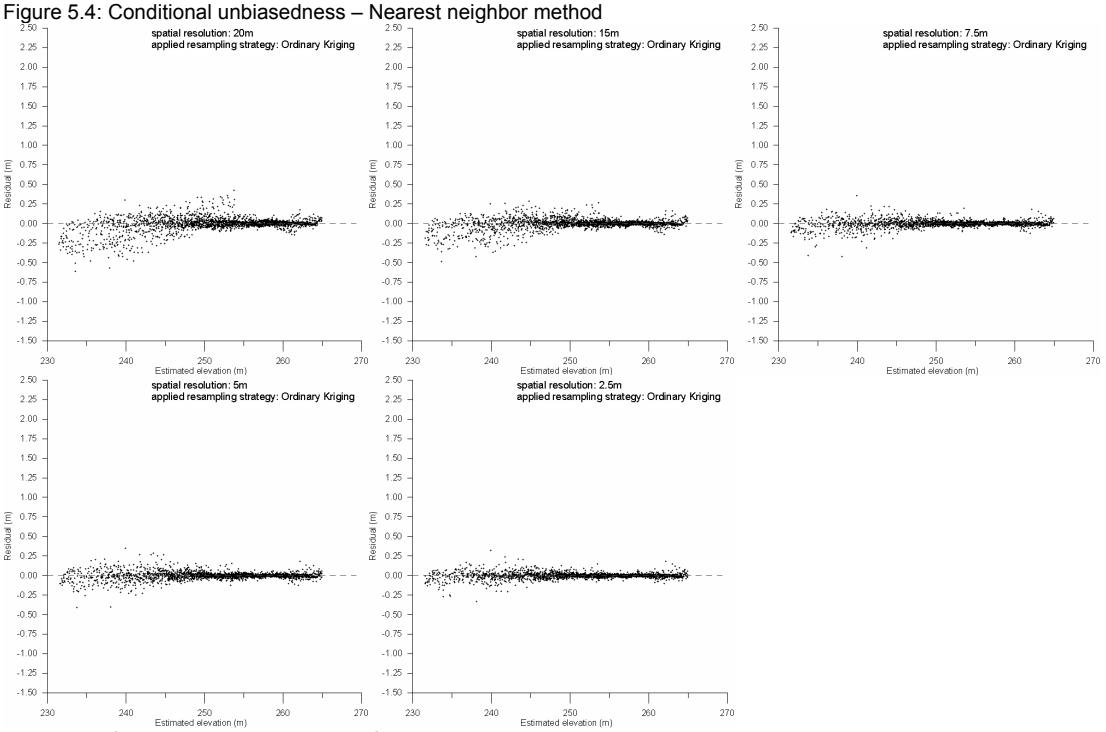

Figure 5.5: Conditional unbiasedness – Ordinary kriging method

The investigation in quality of derived estimates is completed by the visualization of classified residuals on a spatial basis. Six classes were assigned showing an underestimation of true value in red hues and overestimation in blue hues. The classification schema is the same for all three methods which makes the results comparable in magnitude.

The tendency of decreasing magnitude of the residuals can be seen at all three methods when the spatial resolution is increased. This behavior can be explained with the decreasing distance between the location of the sample values and the location of the estimated value. When spatial resolution is increased the weights of the sample values incorporated into the resampling strategy is increased and therefore their influence on the estimate. In other words the estimates derived by the resampling strategy approximate the sample value at the location where the residual is calculated.

Given the inverse distance weight method two areas of divergence are identified. One builds the boarder of the study area, where this method shows overestimation of higher magnitude at the

north and eastern and underestimation of higher magnitude at the southern boarder. Second area is the depthline of the study area where this method shows a higher magnitude of underestimation of true values. The identified areas can be described as areas with less continuity in landscape gradient as areas where the magnitude of over- and underestimation is less. This leads to the conclusion that the applied method should be reinvestigated and the chosen power should be reconsidered. In the actual parameterization the power of two strongly influences nearby sample points and decreases the influence of farther sample points which neglects the incorporation of actual changes in the slope of landscape. If the slope is more continuous this side effect of the applied method does not strongly emerge.

Nearest neighbor method shows some artificial residual patterns at 15m and 7.5m resolution. The smooth surfaces at 5m and 2.5m are due to the nature of the method and again only show that the estimated value approximates the sample value at location where residuals are calculated, but do not provide a global quality assessment tool.

Ordinary kriging method shows the most continuous and smooth residual surface of all applied methods. Again the depthline shows some higher magnitude of underestimation but compared to inverse distance weight method the problem area appears less in size. The areas where inverse distance weight method indicates underestimation of higher magnitude do not appear with ordinary kriging. Regarding the patterns of residuals calculated from the estimates derived by ordinary kriging, the impression of a reasonable surface that reflects reality appears in strong contrast to the surface pattern derived by the nearest neighbor method.

The upcoming two tables summarize the residual analysis broken down to applied resampling strategy and spatial resolution presenting the actual class population.

Table 5.6: Residual class population (%) using decreased spatial resolution

Spatial Resolution	**20m**			**15m**		
Resampling Strategy	**OK**	**IDW**	**NN**	**OK**	**IDW**	**NN**
<-0.350	1.2	9.2	16.7	0.2	5.1	4.7
>-0.350 to -0.175	4.6	7.0	6.0	2.9	8.7	12.6
>-0.175 to 0.000	41.1	37.9	9.8	44.1	39.8	39.4
> 0.000 to 0.175	50.9	34.0	32.3	51.9	36.4	30.2
> 0.175 to 0.350	2.1	6.4	16.8	0.9	5.0	7.8
> 0.350	0.1	5.6	18.4	0.0	5.0	5.2

Table 5.7: Residual class population (%) using increased spatial resolution

Spatial Resolution	**7.5m**			**5m**			**2.5m**		
Resampling Strategy	**OK**	**IDW**	**NN**	**OK**	**IDW**	**NN**	**OK**	**IDW**	**NN**
<-0.350	0.1	3.4	3.1	0.1	0.1	0	0.0	0.0	0
>-0.350 to -0.175	0.7	9.7	5.1	0.7	4.6	0	0.4	0.1	0
>-0.175 to 0.000	48.2	43.3	33.6	49.0	40.5	0	49.3	58.3	0
> 0.000 to 0.175	50.7	33.6	45.1	49.8	51.8	100	50.1	41.5	100
> 0.175 to 0.350	0.4	5.8	10.6	0.5	2.9	0	0.2	0.0	0
> 0.350	0.0	4.2	2.4	0.0	0.2	0	0.0	0.1	0

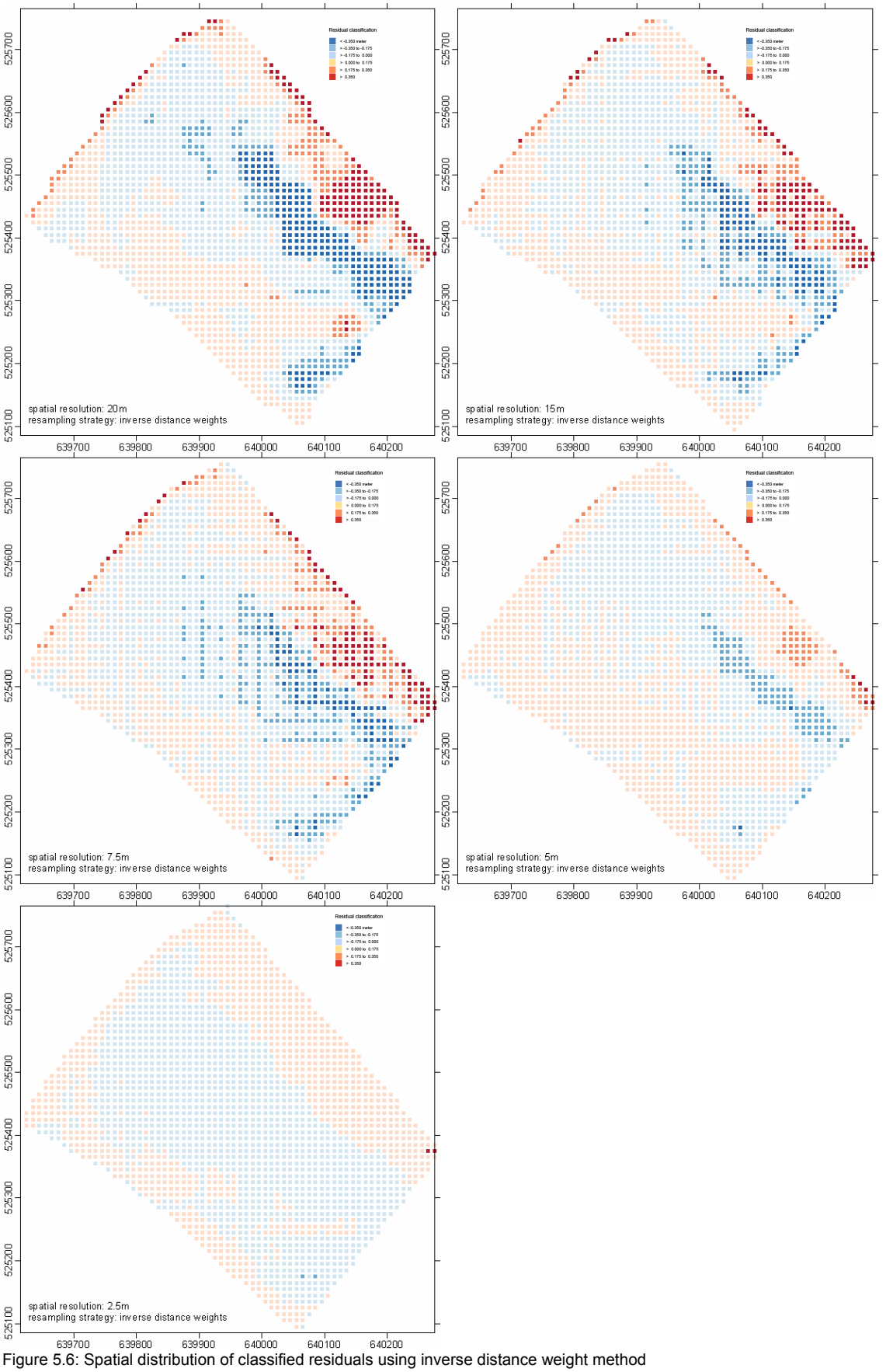

Figure 5.6: Spatial distribution of classified residuals using inverse distance weight method

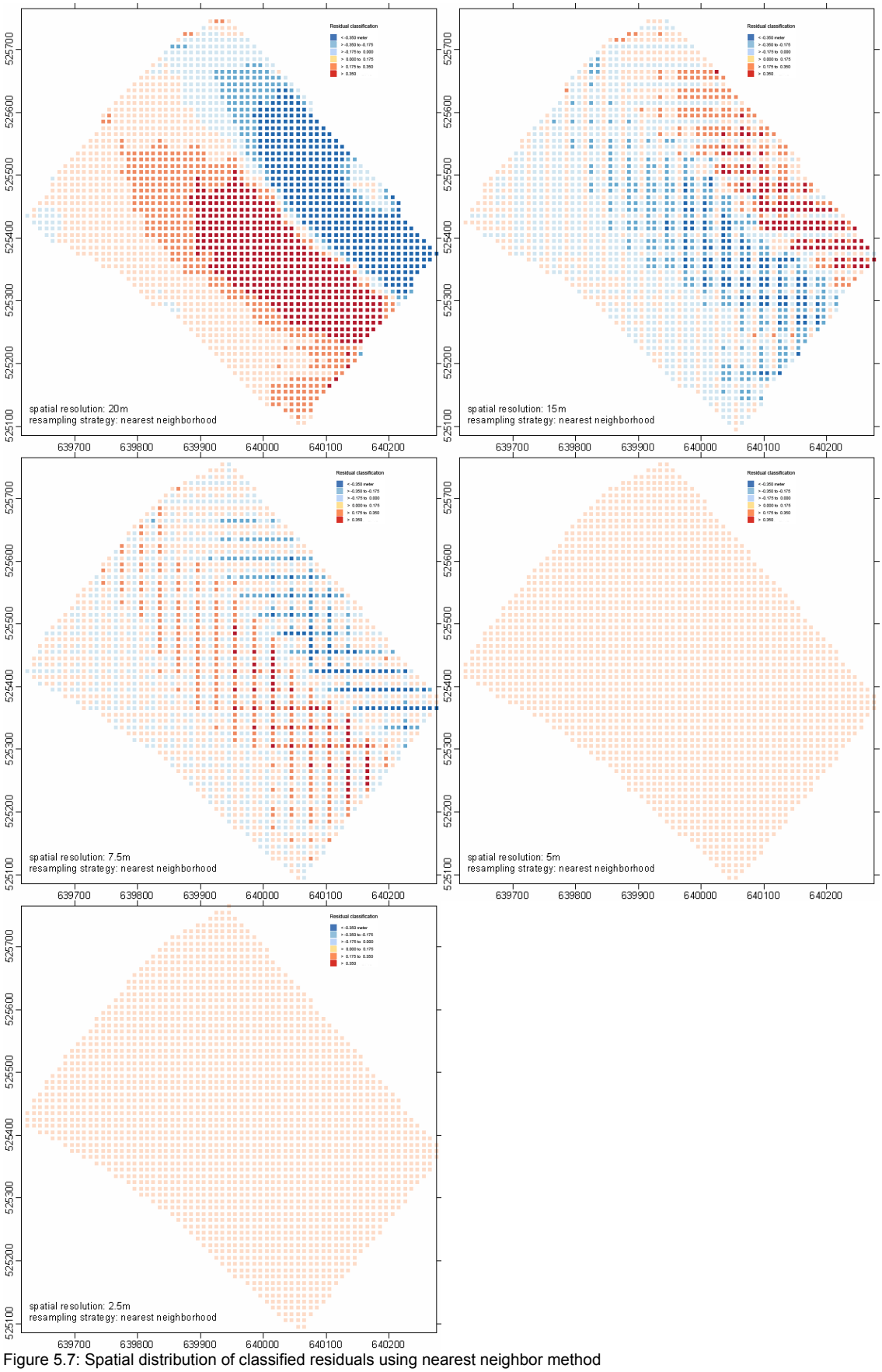

Figure 5.7: Spatial distribution of classified residuals using nearest neighbor method

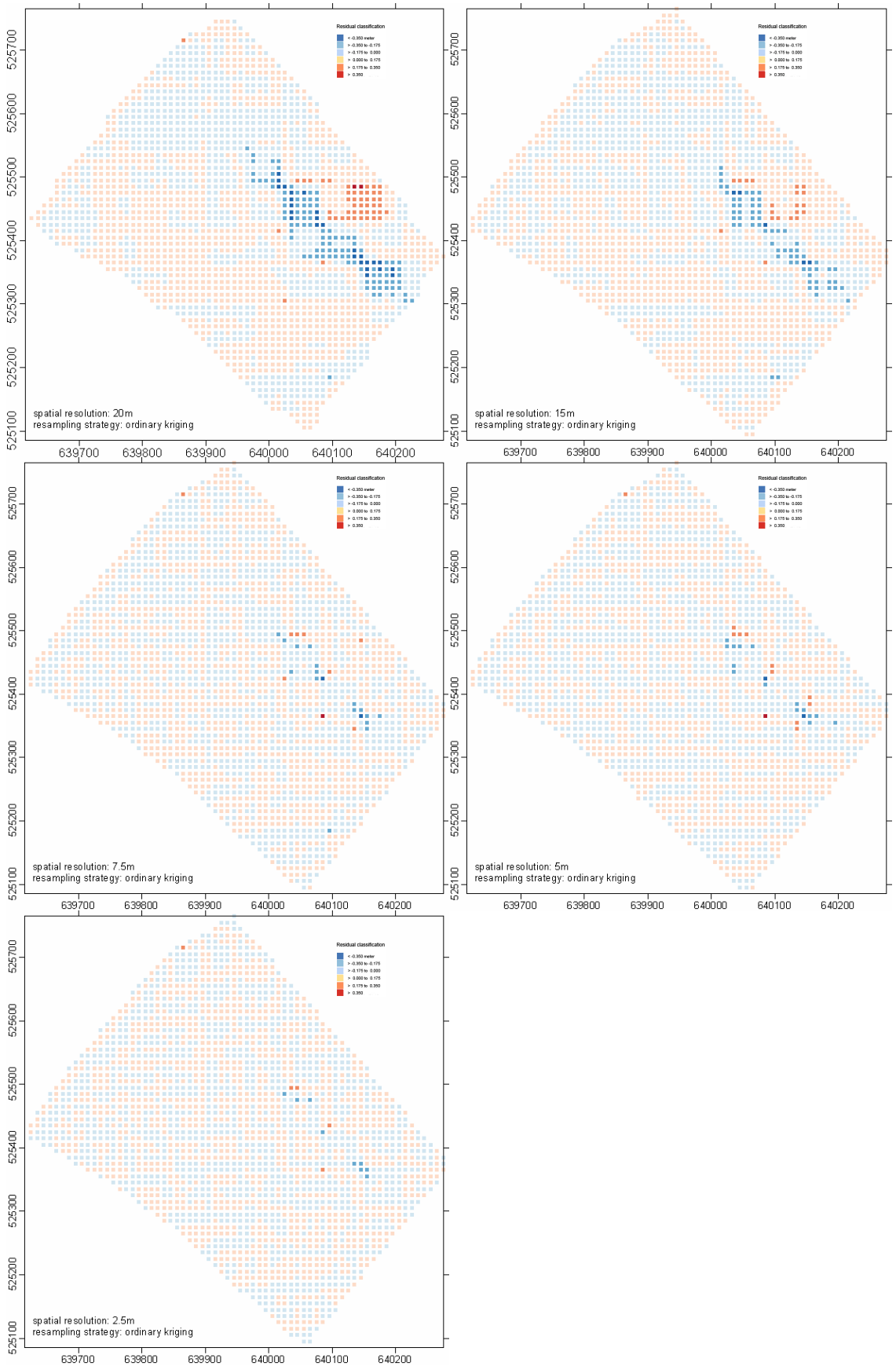

Figure 5.8: Spatial distribution of classified residuals using ordinary kriging method.

Chapter 6

Analysis of GeoWEPP results

6.1 Analysis on hillslope level

All upcoming results were derived the following way. The resampled digital elevation models using either inverse distance weight method, nearest neighbor method or ordinary kriging method to derive spatial resolutions of 20m, 15m, 7.5m, 5m and 2.5m were joined with the comprehensive input dataset of WEPP (assembled separately) resulting in 15 watershed models. The so called native watershed model was formed by the same comprehensive input dataset and the DEM of 10m spatial resolution. All upcoming analysis compares the results calculated from the 15 watershed models with the results from the native watershed model.

Values for the critical source area (CSA) and the minimum source channel length (MSCL), those are required input parameters of TOPAZ to delineate the watershed were assigned 0.83ha and 75m respectively because those values gave a realistic (based on experiences) representation of the study site (Figure 6.6). A detailed overview of the watershed segmentation can be found at Table 6.1 and Table 6.2 also including the other investigated resampling strategies.

These tables accommodate parameters that are derived through the segmentation process of TOPAZ. The identified channels and hillslopes within the watershed are accumulated to identified segments. These segments form the area of the watershed that can be easily calculated regarding spatial resolution of the digital elevation model and TOPAZ output files. The computational time is recorded at each run and may vary between different processor types but is consistent within the given setup of this study.

Table 6.1: Subwatershed statistics using decreased spatial resolution

Spatial Resolution		**20m**			**15m**	
Resampling Strategy	**OK**	**NN**	**IDW**	**OK**	**NN**	**IDW**
Identified Segments	15	17	15	15	20	19
Watershed Area (ha)	12.68	12.80	12.56	14.29	13.97	14.02
Computational Time (mm:ss)	00:30	00:32	00:29	00:43	00:57	01:03
Hillslopes	11	12	11	11	14	13
Footpaths	61	63	63	96	143	132
Channels	4	5	5	4	6	6

Table 6.2: Subwatershed statistics using increased spatial resolution

Spatial Resolution	7.5m			5m			2.5m			10m
Resampling Strategy	**OK**	**NN**	**IDW**	**OK**	**NN**	**IDW**	**OK**	**NN**	**IDW**	**native**
Identified Segments	10	16	18	17	4	24	11	11	32	17
Watershed Area (ha)	15.97	15.64	15.69	17.18	15.86	16.75	17.80	16.60	17.85	15.11
Computational Time (mm:ss)	02:24	05:23	03:13	07:21	14:32	13:21	43:43	22:40	52:59	01:14
Hillslopes	7	11	13	12	3	17	8	8	23	12
Footpaths	350	814	484	1024	2228	2118	6258	3411	8511	173
Channels	3	5	5	5	1	7	3	3	9	5

At first glance it becomes obvious that outlined parameters vary between different resolutions as well as within the same resolution derived by different resampling strategies. Given 17 identified segments at 10m resolution the model results at 2.5m (IDW) showed 32 identified segments which is almost twice as much. The same relation can be found by the identified channels at the native digital elevation model and the resampled digital elevation model of 2.5m (IDW). For all these comparisons it is important to keep in mind that the parameterization was the same for all investigated cases except the spatial resolution of the digital elevation model.

The increase of computational time corresponds with the increase of spatial resolution which seems reasonable since the number of cells incorporated into the digital elevation model increases. The same might be true for the number of flowpaths. Interestingly the area of the modeled watershed reaches from about 12.5ha at low spatial resolution to almost 17.8ha at high spatial resolution while the 10m digital elevation model outlines an area of about 15ha which falls in the middle of the maximum and minimum.

The segmented watershed includes the blue fluctuant lines representing the identified channels while the colorful shapes represent the identified hillslopes that reside adjacently or on top of the channel. Despite the segmentation TOPAZ calculates various output files that build the basis for the successful simulation run of WEPP model.

The upcoming overview of delineated watersheds is based on DEMs resampled through the application of the ordinary kriging method. The watershed with a spatial resolution of 10m (2nd row on left side) is derived from the native digital elevation model.

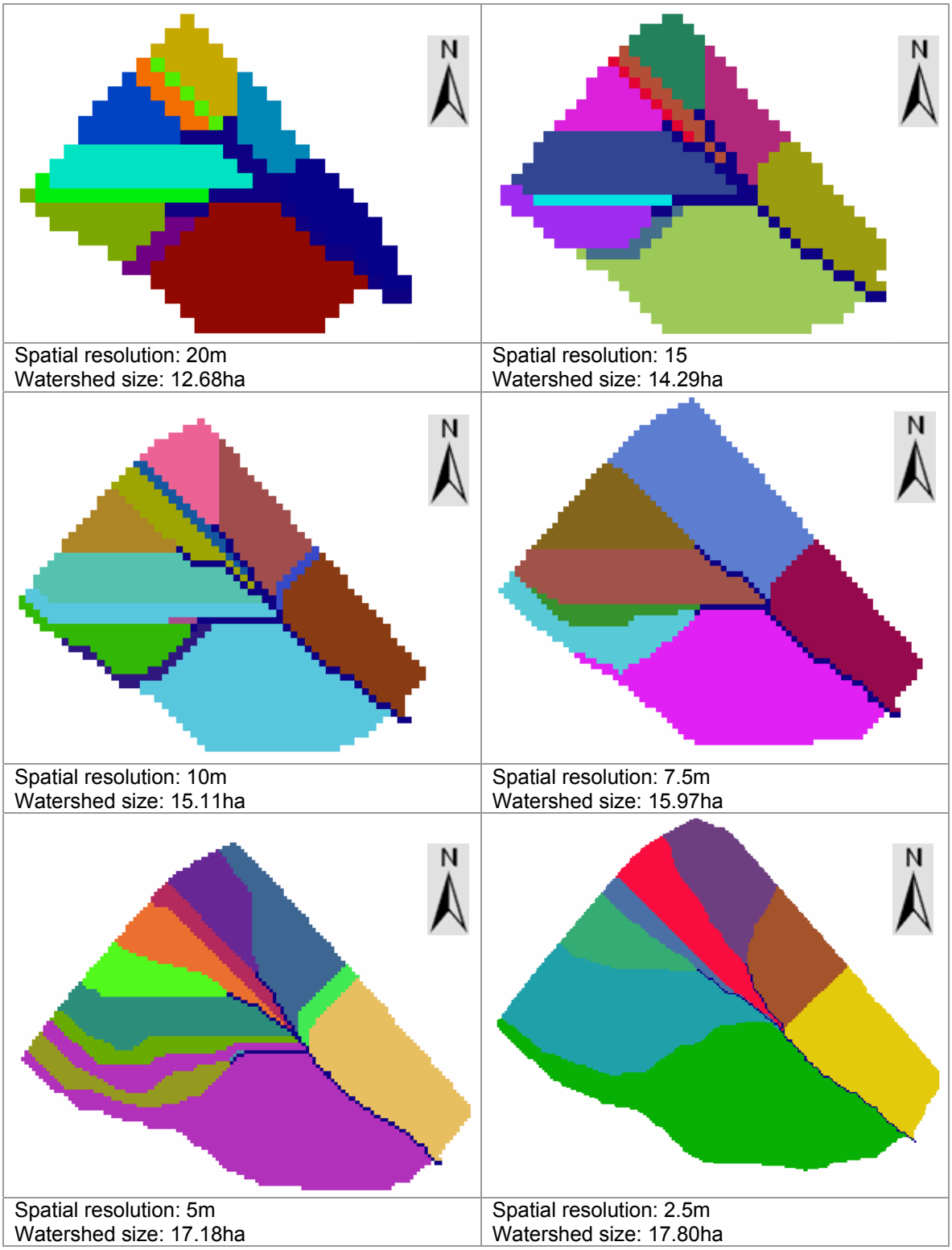

Figure 6.1: Watershed delineation derived from DEMs resampled by ordinary kriging method

Despite the segmentation of the watershed TOPAZ calculates additional parameters like slope of flow vector. Important to mention is that the slope values derived by TOPAZ represent an unit less value and must not be mixed up with slope values derived by any other slope algorithm. The normalized histogram visualization of derived slope values is presented next.

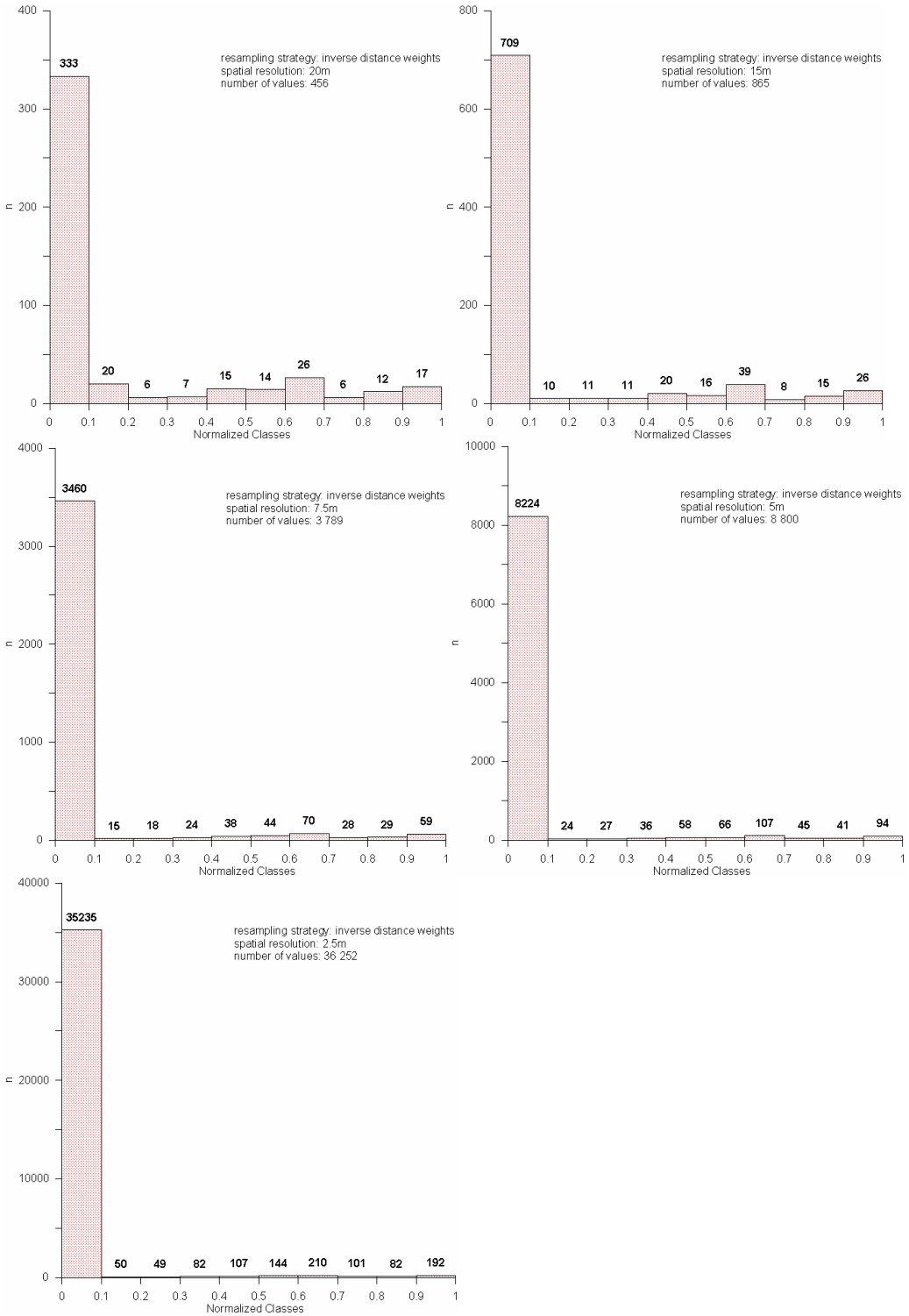

Figure 6.2: Histogram of slope values derived by TOPAZ from DEMs resampled by IDW

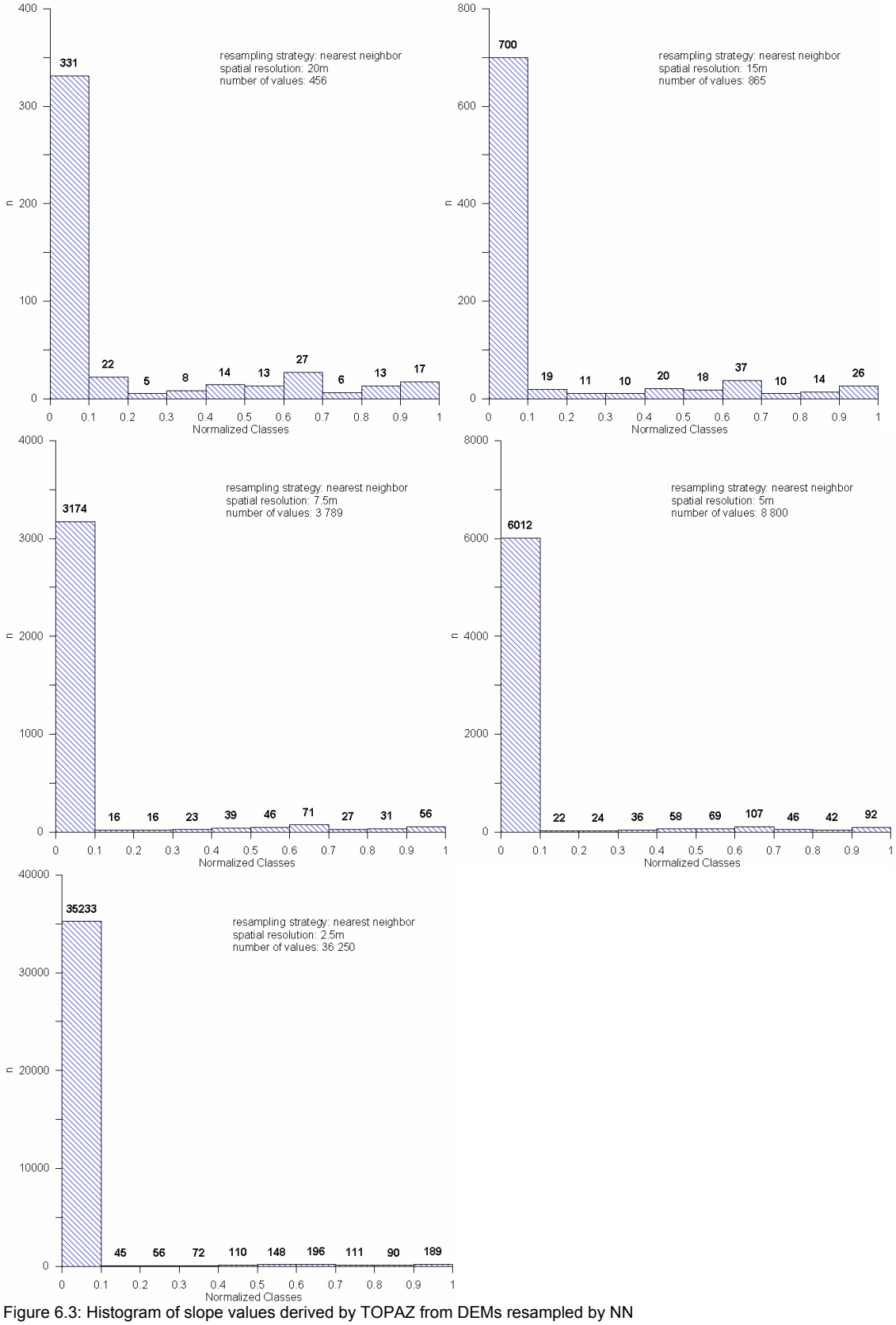

Figure 6.3: Histogram of slope values derived by TOPAZ from DEMs resampled by NN

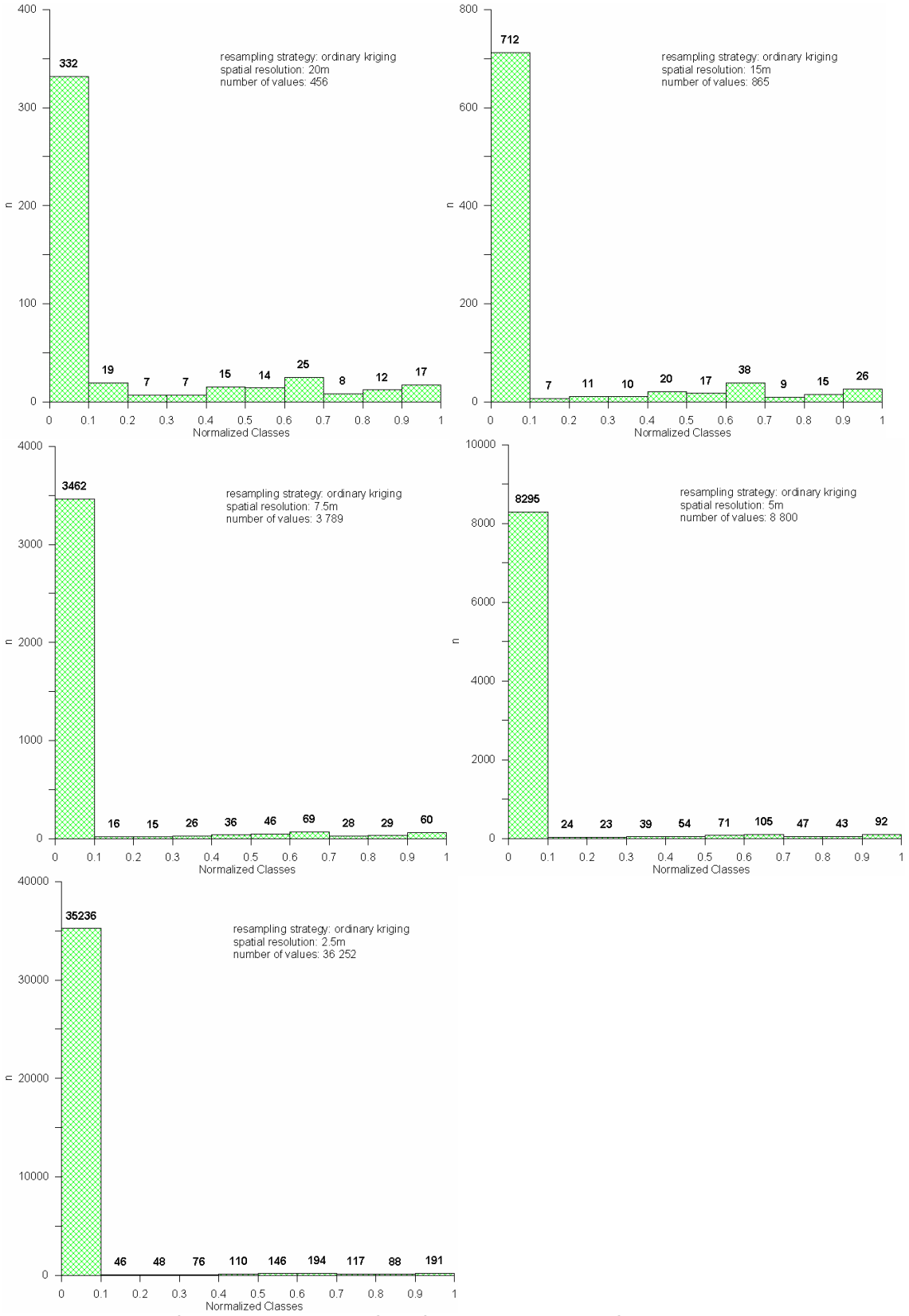

Figure 6.4: Histogram of slope values derived by TOPAZ from DEMs resampled by OK

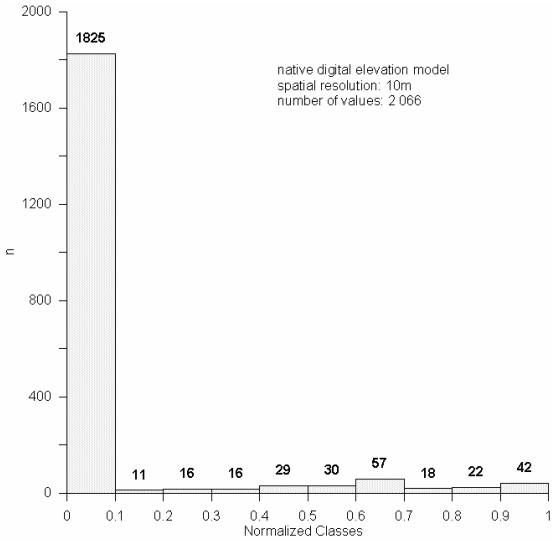

Figure 6.5: Histogram of slope values derived by TOPAZ from native DEM

Investigating at these histograms it becomes obvious that class one reaching from 0 to 0.1 increases its population on the cost of the other classes when spatial resolution increases. Although absolute numbers may lead to different interpretation, taking the total number of values into account this assumption seems to be supported. In simplified words, there is a shift of class population from high slope values to low slope values observable. These observations are summarized by the following tables.

Table 6.3: Statistics of calculated slope (unit less) using decreased spatial resolution

Spatial Resolution		**20m**			**15m**		**10m**
Resampling Strategy	**IDW**	**NN**	**OK**	**IDW**	**NN**	**OK**	**native**
Number of values	456	456	456	865	865	865	2066
Mean	0.305	0.314	0.311	0.311	0.315	0.316	0.321
Standard deviation	0.439	0.448	0.446	0.539	0.544	0.546	0.710
Variance	0.193	0.201	0.199	0.291	0.296	0.299	0.504
Coefficient of variation	1.442	1.427	1.433	1.735	1.728	1.732	2.214
Minimum	0.018	0.014	0.011	0.005	0.005	0.009	0.007
First quartile	0.065	0.065	0.065	0.060	0.052	0.061	0.057
Median	0.090	0.095	0.092	0.085	0.087	0.087	0.421
Third quartile	0.191	0.195	0.200	0.146	0.156	0.141	0.127
Maximum	1.640	1.665	1.660	2.213	2.227	2.233	3.390
Range	1.622	1.651	1.649	2.209	2.222	2.224	3.383

Table 6.4: Statistics of calculated slope (unit less) using increased spatial resolution

Spatial Resolution		**7.5m**			**5m**			**2.5m**		**10m**
Resampling Strategy	**IDW**	**NN**	**OK**	**IDW**	**NN**	**OK**	**IDW**	**NN**	**OK**	**native**
Number of values	3789	3789	3789	8800	8800	8800	36252	36250	36252	2066
Mean	0.318	0.327	0.321	0.323	0.333	0.322	0.328	0.341	0.326	0.321
Standard deviation	0.834	0.840	0.840	1.045	1.054	1.054	1.514	1.528	1.530	0.710
Variance	0.696	0.705	0.706	1.092	1.111	1.111	2.292	2.336	2.341	0.504
Coefficient of variation	2.620	2.567	2.617	3.232	3.163	3.270	4.617	4.483	4.687	2.214
Minimum	0	0	0	0	0	0	0	0	0	0.007
First quartile	0.053	0.047	0.053	0.042	0	0.042	0.040	0	0.040	0.057
Median	0.080	0.093	0.080	0.080	0.080	0.080	0.080	0	0.080	0.421
Third quartile	0.120	0.141	0.123	0.120	0.160	0.113	0.120	0.200	0.113	0.127
Maximum	4.520	4.560	4.547	6.820	6.860	6.860	13.720	13.760	13.760	3.390
Range	4.520	4.560	4.547	6.820	6.860	6.860	13.720	13.760	13.760	3.383

The number of total slope values increases as spatial resolution increases. Parallel to this increase the range of slope values increases too. Mean shows a slight increase with increase of spatial resolution so does variance. Median value is remarkable lower at all spatial resolutions than median value of native 10m resolution and median values are constantly lower than mean values indicating a positive skewness of the distribution. Hence the distribution of slope values is asymmetric leading to the conclusion that numerous slope values with lower magnitude contribute to the distribution. On the other hand these values are balancing a few slope values of higher magnitude.

GeoWEPP uses the watershed segmentation for further analysis and finally for the calculation of magnitude of surface runoff, sediment yield, erosion and deposition as well as the spatial erosion and deposition pattern. The visualization of the spatial erosion and deposition builds on the concept of a threshold value called “tolerable soil loss/target value (T)” which is by default one (t/ha/year) and can be changed according to investigated purposes.

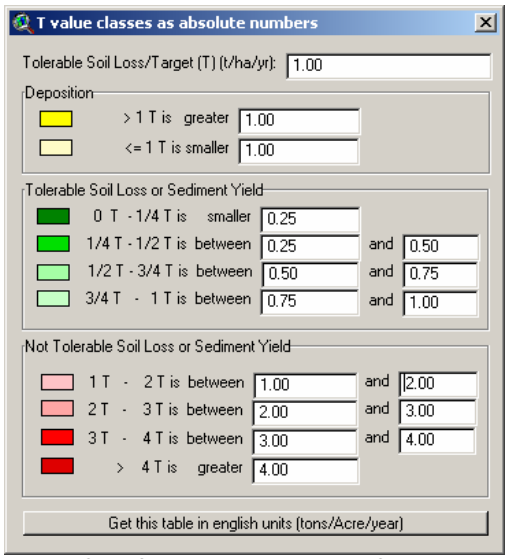

Figure 6.6: Classification according to specified tolerable soil loss value

Relating to Figure 6.6 the T value leads to three major classes. Firstly the deposition class holding all deposition values, secondly the class of tolerable soil loss and sediment yield and thirdly the class of intolerable soil loss and sediment yield. All three classes hold subclasses in order to provide a more detailed view on each individual class leading to a total of 10 individual classes.

The T value was left unchanged for this study defining class borders according to Figure 6.7. The upcoming graphs show the area of the watershed affected by each single class compared to the affected area derived by the usage of DEM’s native spatial resolution of 10m. In other words class two represents areas where deposition is equal or smaller than one tonne per hectare and year. Class three is presented in a separate graph at the end of the following figures section due to the magnitude of affected area.

Concerning all different spatial resolutions as well as all different resampling strategies one common feature of all plots is that they present the same classes populated. This means that there was no simulation run leading to outliers in terms of severe erosion or deposition. Interesting to observe is the fact, that only at class three regarding spatial resolutions of 7.5m, 5m and 2.5m the area affected by erosion yielded from resampled digital elevation models was higher than erosion affected area at native digital elevation model. At all other spatial resolutions as well as resampling strategies the native area affected by erosion was higher than erosion affected area at resampled digital elevation models. Regarding deposition affected area there is the tendency observable that native deposition area is overestimated with a decrease of DEM's spatial resolution.

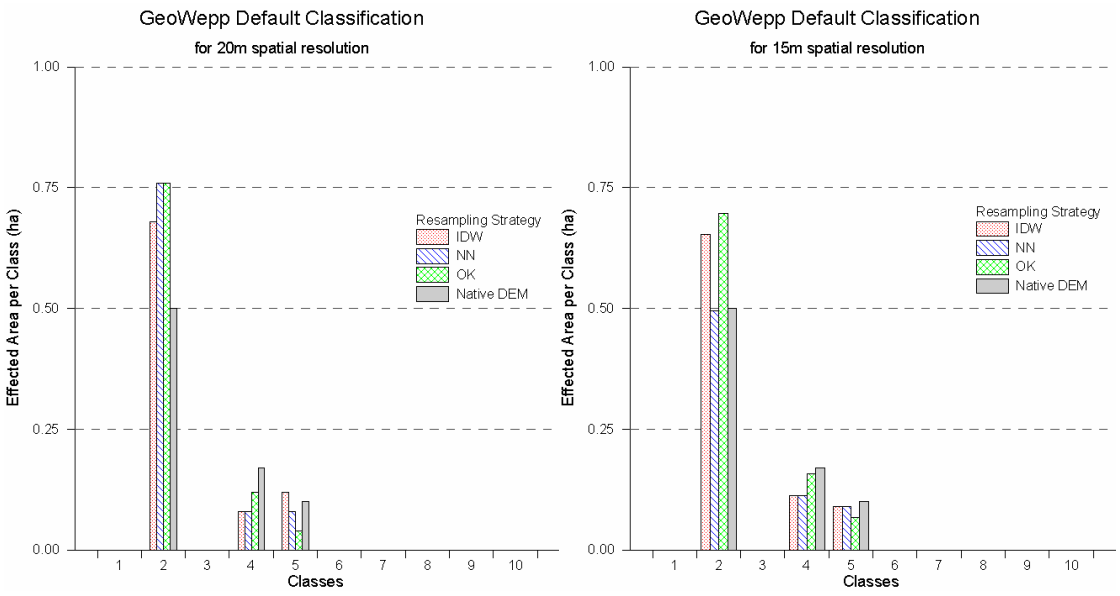

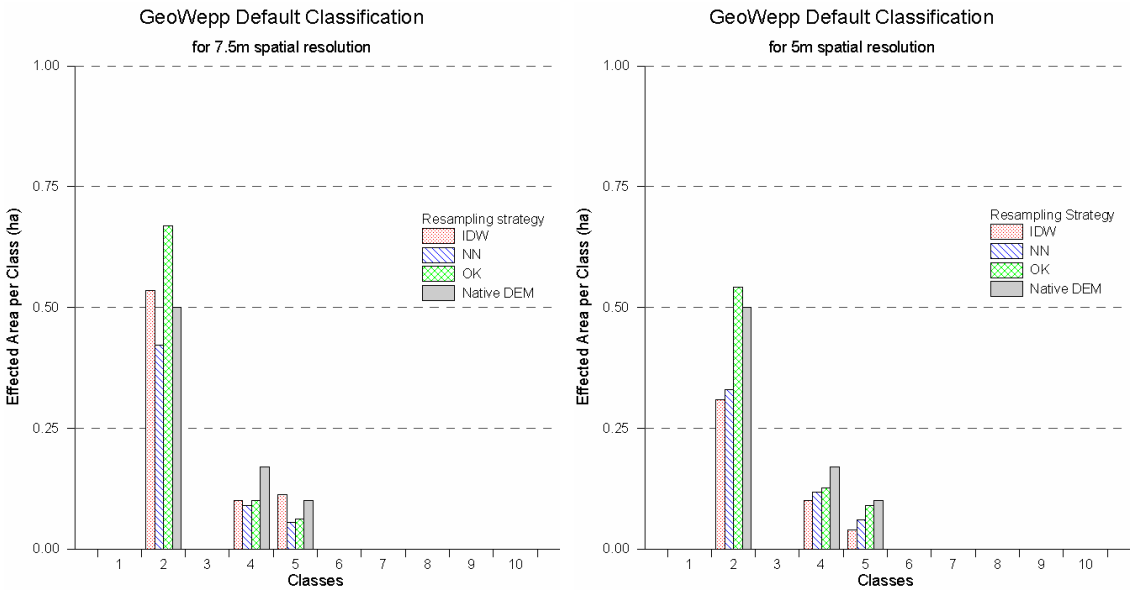

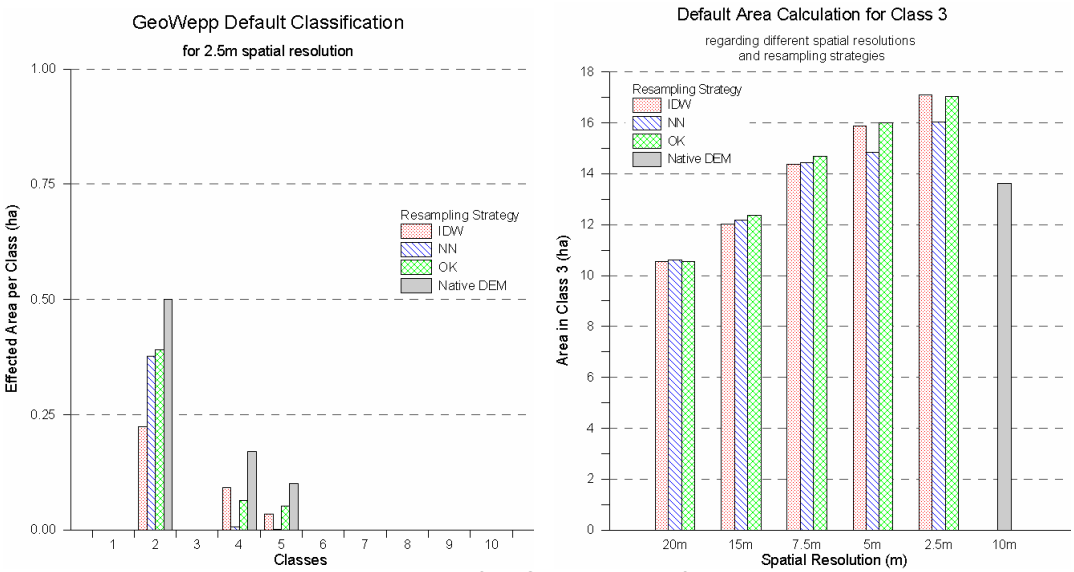

Figure 6.7: Area occupied per class according to default GeoWEPP classification

The upcoming two graphs display the area affected by erosion and deposition processes within the watershed according to the applied resampling strategy and the investigated spatial resolution.

The conclusion that can be drawn in case of erosion processes is that an increase in the spatial resolution of the digital elevation model leads to an overestimation of area affected by erosion while a decrease in spatial resolution behaves oppositely. In case of area affected by deposition processes the situation differs slightly from that of erosion processes. A trend of an increase in area affected by deposition linked to a decrease of DEM's spatial resolution can be observed by all three different resampling strategies although the magnitude of increase varies between applied resampling strategies. Concerning spatial resolutions of 5m and 2.5m the area affected by deposition is underestimated (excluding two results). An overestimation can be seen at all other spatial resolutions in case of DEMs resampled by IDW and OK while results derived from DEMs resampled by NN consistently (excluding one result) underestimates the area affected by deposition.

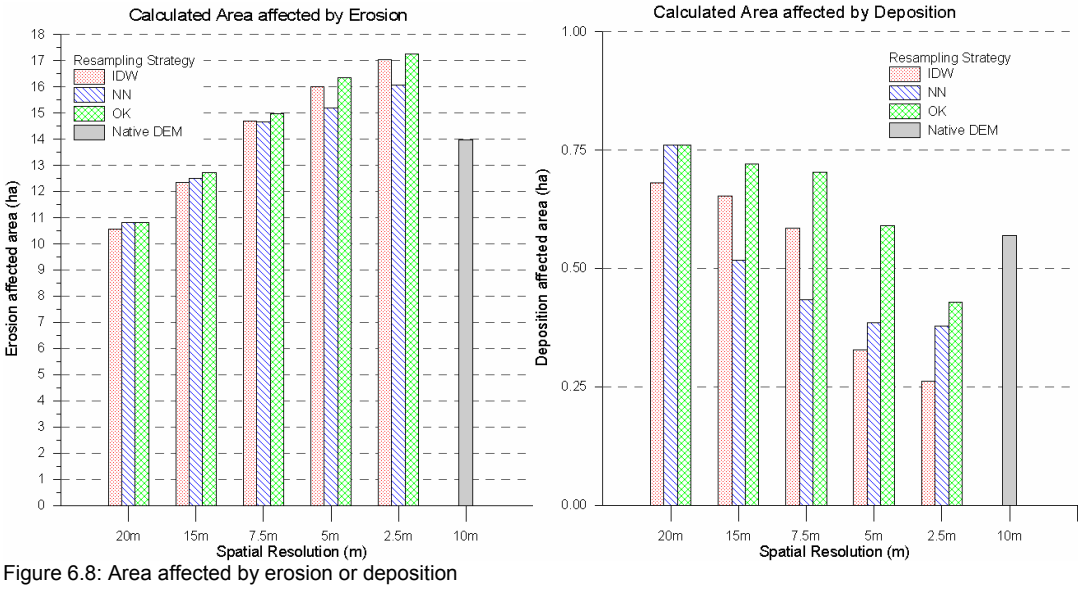

Figure 6.8: Area affected by erosion or deposition

Table 6.5 summarizes the magnitude of differences in size of area occupied by erosion and deposition processes broken down to all investigated spatial resolutions and resampling strategies and again compared to calculated area at a spatial resolution of 10m.

Table 6.5: Absolute differences in area size

	Absolute differences in area size (ha)					
	area affected by erosion			**area affected by deposition**		
Spatial Resolution	**IDW**	**NN**	**OK**	**IDW**	**NN**	**OK**
20m	-3.21	-3.17	-3.17	0.11	0.19	0.19
15m	-1.64	-1.48	-1.26	0.08	-0.05	0.15
7.5m	0.72	0.70	0.99	0.02	-0.14	0.13
5m	2.13	1.21	2.36	-0.24	-0.19	0.02
2.5m	3.41	2.08	3.30	-0.31	-0.19	-0.14

At first glance the presented values clearly show a trend of underestimation of erosion affected areas at decreased spatial resolutions and an overestimation at increased spatial resolutions. This trend can also be found in case of deposition affected areas but with an opposite behavior showing an overestimation at decreased spatial resolutions and an underestimation at increased spatial resolutions. Necessary for a rating of the outlined magnitudes are the reference values derived from the 10m spatial resolution. The native area affected by erosion processes showed a value of 13.97ha while the area affected by deposition processes showed a value of 0.57ha.

Relative differences regarding the occupied area with either process are displayed by the following graphs. Graph with diamonds marker symbols from upper left to lower right corner indicates relative differences concerning deposition affected area, graph with cross marker symbols form lower left to upper right corner presents the relative differences of area affected by erosion and continuous graph without marker symbols indicates the difference of total watershed size again compared to values derived from 10m spatial resolution.

At first glance the shape of graphs for IDW and OK are similar while the graphs with cross marker symbols are more similar than the graphs with diamonds marker symbol. Again the conclusion that an increase in spatial resolution leads to an overestimation of area affected by erosion and to a severe underestimation of deposition affected area is supported. This tendency is also reflected in case of NN resampling strategy although the shape of the graphs indicating differences of deposition affected area strongly differs. Important to note is that the watershed size also varies leading to the statement that ideally the blue and the red line would coincide.

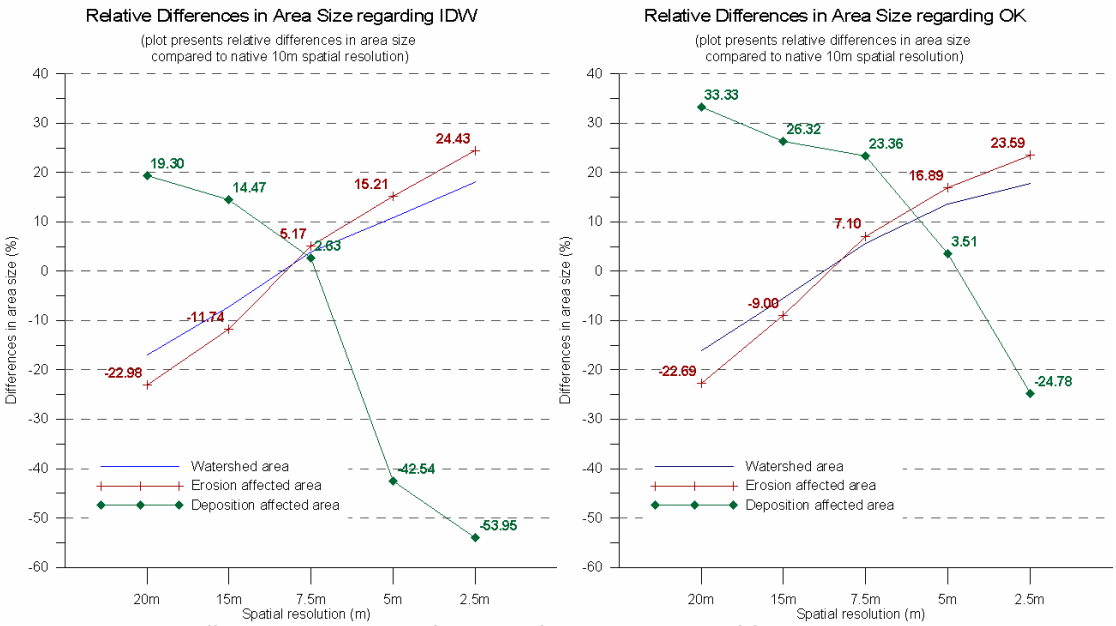

Figure 6.9: Relative differences in area size (left: in case of IDW; right: in case of OK)

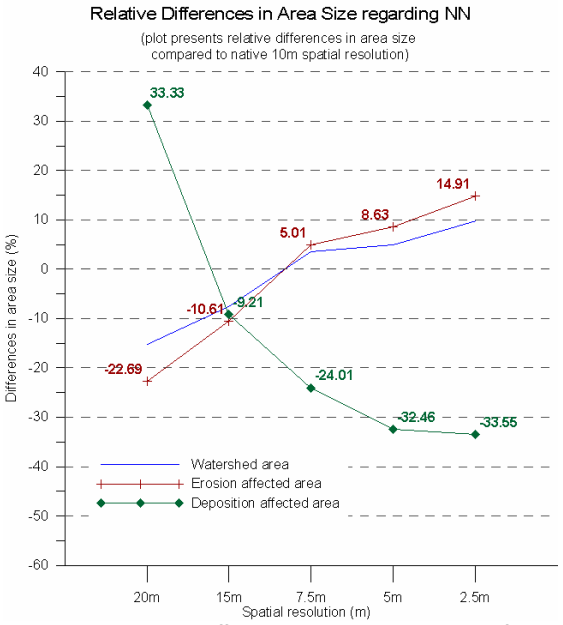

Figure 6.10: Relative differences in area size in case of NN

For the investigated year 2003 the model calculated two erosive events for hillslopes namely on the 17th of July and on the 31st of December. The accumulated runoff from all hillslopes broken down to the different spatial resolutions is presented for both events. Concerning runoff there are only two situations where runoff values are below the value derived from 10m spatial resolution. Once at 5m spatial resolution of about 50% on 17th of July and once at 20m spatial resolution of about 40% on 31st of December. All other calculated runoff values exceed the reference value on average 2.2 (±1.51) times or by maximum 7.5 times.

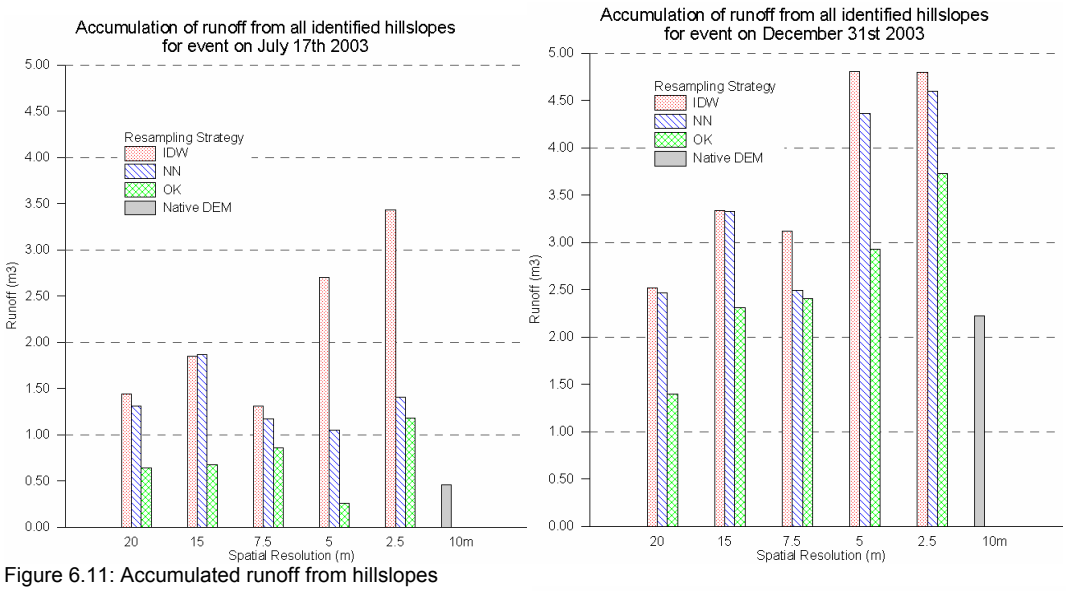

Figure 6.11: Accumulated runoff from hillslopes

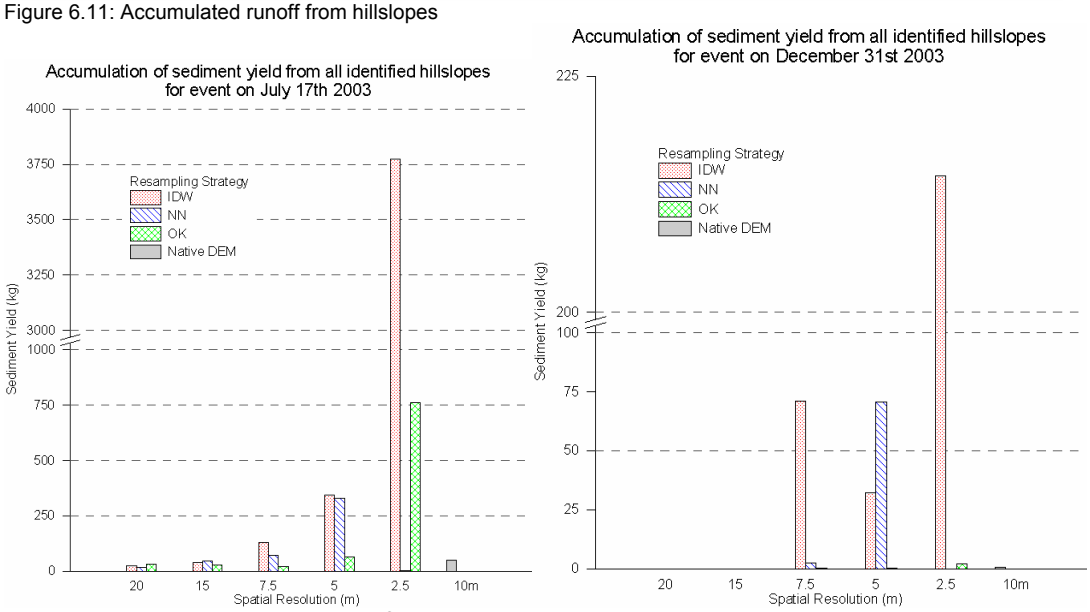

Figure 6.12: Accumulated sediment yield from hillslopes

Investigating the situation of sediment yield on hillslope level for both events the results are much more diverging than in case of runoff. The outlier values at 2.5m spatial resolution would need further treatment for a secured assessment because the presented values really seem to be unrealistic. Regarding the other sediment yield values in case of July event the reference value is overestimated in 7 cases, for December event in 6 cases taking a total of 15 values leads to the conclusion that overestimation occurred in 46% respectively 40% of all investigated cases. Absolute values show that overestimation varies between 1.3 and 15 times for July event and 3.1 to 100 times for December event while underestimation reaches from 6% to 96% for July event and from 60% to 100% for December event. These values clearly indicate that there is a lot of variance included in sediment yield values calculated by the simulation.

6.2 Analysis on watershed level

So far the analysis of GeoWEPP results was focused on the hillslope level. The second part of analysis deals with the calculated results for watershed level. The analysis starts with the summary of precipitation depth (mm) and sediment yield (kg) for the investigated watershed. Remarkable about the event frequency is that an additional event on 30th of December is predicted that did not appear at hillslope level. Runoff volume and peak runoff volume as well as the sediment yield of this event are almost identical to the values derived from 10m spatial resolution. Due to this high amount of agreement this event is not analyzed into more detail.

The values for precipitation depth and sediment yield are almost consistent at all investigated resampling strategies and spatial resolutions. Nevertheless at two cases a sediment yield at watershed outlet was reported, once at application of inverse distance weight method at 15m spatial resolution with 3.7kg and once at the application of nearest neighbor method at 5m spatial resolution with 3.3kg.

Table 6.6: Sediment yield and precipitation depth at watershed outlet

	Precip. Depth (mm)			Sed. Yield (kg)		
Date	**17.07**	**30.12**	**31.12**	**17.07**	**30.12**	**31.12**
20m	28.7	8.5	12.2	0	0	0
15m	28.7	8.5	12.2	3.7(*)	0	0
10m	28.7	8.5	12.2	0	0	0
7.5m	28.7	8.5	12.2	0	0	0
5m	28.7	8.5	12.2	3.3(**)	0	0
2.5m	28.7	8.5	12.2	0	0	0

* observed by application of IDW method

** observed by application of NN method

The situation for runoff volume and peak runoff volume appears differently. While again results from inverse distance weight method and ordinary kriging method show similar behavior with a different magnitude of values, nearest neighbor method strongly differs. The following graphs show on left side runoff volume values and on right side peak runoff volume values. The dashed line symbolizes the reference value derived from 10m spatial resolution. One obvious observation is the similarity of runoff volume graph and peak runoff volume graph.

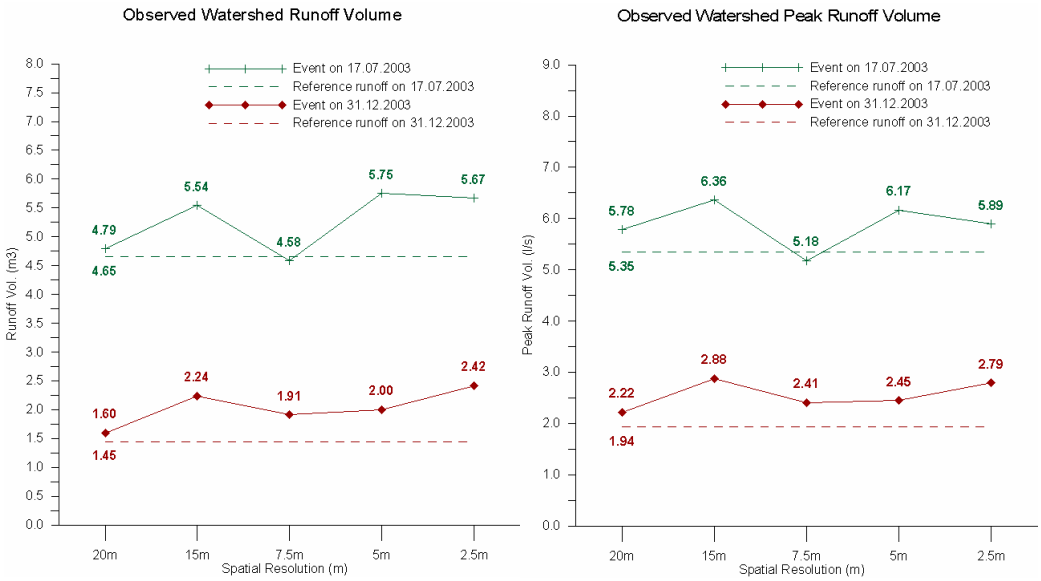

Figure 6.13: Runoff and peak runoff values derived from DEMs resampled by IDW method

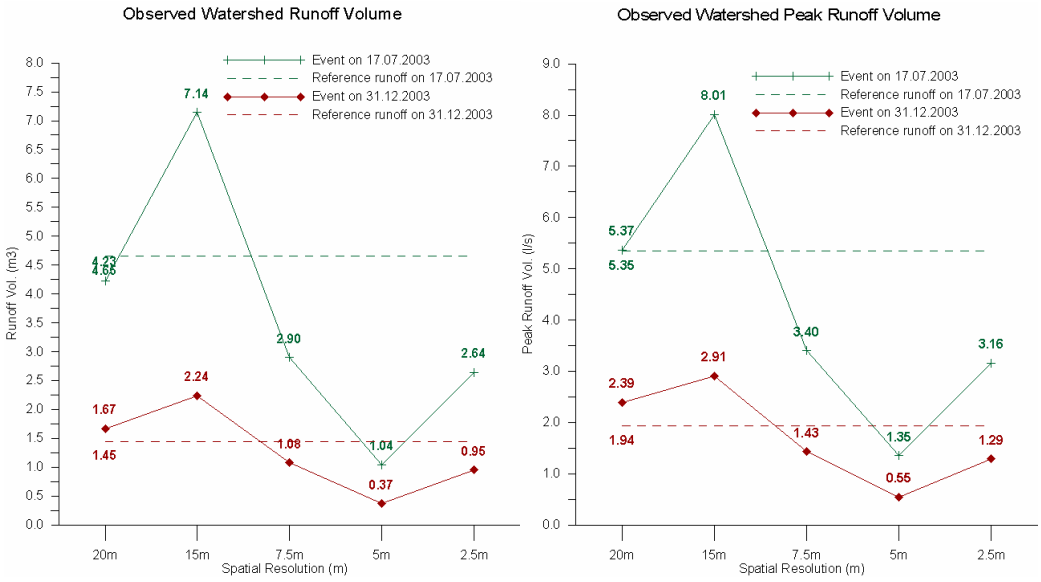

Figure 6.14: Runoff and peak runoff values derived from DEMs resampled by NN method

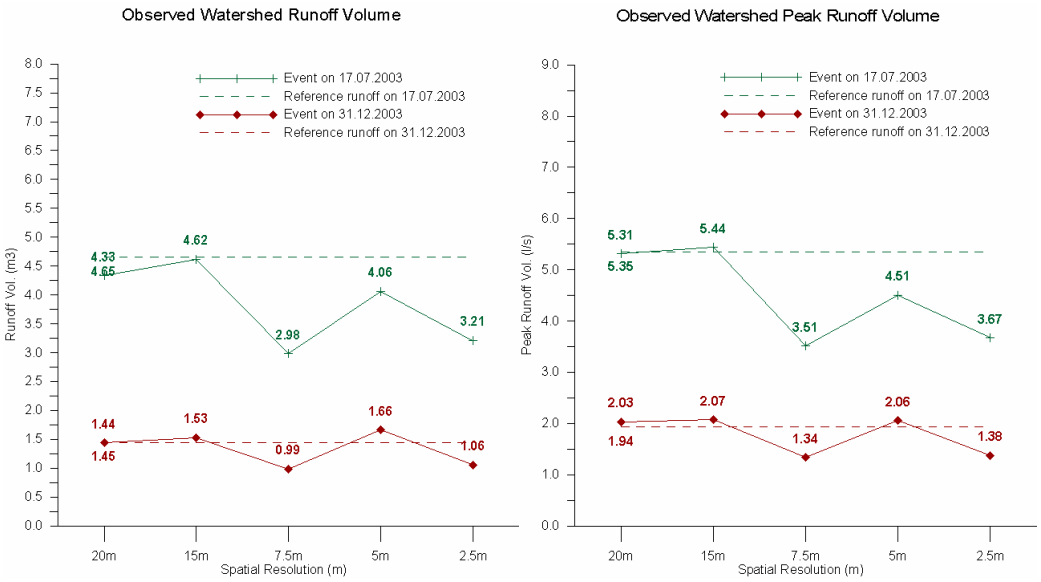

Figure 6.15: Runoff and peak runoff values derived from DEMs resampled by OK method

Analyzing the presented graphs in more detail it seems that runoff is overestimated (taking the 15 calculated results) at 87% with inverse distance weight method, at 27% with nearest neighbor method and at 47% with ordinary kriging method. The presented numbers are based on a very small sample size indicating some included uncertainty. This leads to the fact, that the outlined percentages describe the calculated values and do not favor a general trend. The situation of overestimation appears similar with peak runoff volume values showing 87% overestimation with inverse distance weight method, 33% with nearest neighbor method and 53% overestimation with ordinary kriging method.

Chapter 7

Summary

This study presented the simulation results for soil erosion, surface runoff and sediment yield by using the GeoWEPP model for an agriculturally used watershed in Mistelbach Lower Austria. This investigated watershed is 22.3ha of size, reaches from about 230m to 265m of elevation and shows a mean slope of 8.1% (± 4.3%).

The erosion model was run for the year 2003, which was a dry year with an annual rainfall total of 395.8 mm compared to an eleven years time series (between 1994 and 2004) with an average annual total of 659mm (±129mm). The erosion model was parameterized according to the actual conditions observed at study site. This means that the necessary management file reflected the crop cycle apparent in 2003, the necessary soil input file reflected the soil properties derived by sampling campaigns as well as from the official Austrian soil map. The assembled climate input file reflected the observed climate conditions for the year 2003. Two rainfall events were remarkable over the investigated period, namely one event on 17th of July with a total of 28.7mm and a second event on 5th of October with a total of 28.5mm.

The necessary terrain characteristics were derived from a DEM with a spatial resolution of 10m which was considered as the best available estimation of reality and built the reference DEM for further analysis. The spatial resolution of the reference DEM was increased as well as decreased by the application of three different resampling strategies namely the nearest neighbor method, inverse distance weight method and the ordinary kriging method. The increase of spatial resolution yielded to DEMs incorporation a spatial resolution of 7.5m, 5m and 2.5m while the decrease produced DEMs representing spatial resolutions of 15m and 20m.

All the resampled DEMs plus the native DEM of 10m spatial resolution together with the necessary WEPP inputfiles were joined to create a total of 16 different watershed models. GeoWEPP was run for each individual watershed model and simulation results derived from the watershed models incorporating the resampled DEMs were compared with the simulation results derived from the native DEM.

The analysis of simulation results showed, that the calculated area affected by erosion processes increased consistent with all resampling strategies when spatial resolution of the digital elevation model was increased while the affected area decreased with a decrease of DEM's spatial resolution.

Regarding the area size affected by deposition processes an inverse observation was made. A decrease in DEM's spatial resolution lead to an increase in deposition affected area while an increase in DEM's spatial resolution showed a reduction in the area size which was affected by deposition processes.

The analysis of accumulated runoff from hillslopes for both events (17th of July and 31st of December) showed a tendency of overestimation supported by the fact that this observation was made at 87% of all calculated runoff values. There were only two cases where simulation results were below the reference runoff value. Regarding the runoff of all events the calculated runoff value was on average 2.2 (± 1.51) times higher than the reference value. Investigating on sediment yield from hillslopes the rate of overestimation was much smaller. 46% of calculated sediment yield values for the event on 17th of July and 40% of values for event on 31st exceeded the reference value. The presented values support the observations made during this study and are not supposed to be generalized based on the relatively small sample size (n=30).

Observations made during the analysis referring to the watershed were as follows: the calculated sediment yield values consistently (with two exceptions) reported no sediment yield from this watershed. The investigated values of runoff volume showed an overestimation of 87% applying inverse distance weight method, 27% with nearest neighbor method and finally 47% with ordinary kriging method. Calculated peak runoff values showed the similar trend with different magnitude. Using inverse distance weight method reference value was overestimated of about 87%, 33% in case of nearest neighbor and 53% with the application of ordinary kriging.

Regarding all observations made during this study it became obvious that DEM's spatial resolution should be cautiously considered when applying GeoWEPP model for erosion simulation purposes. A specific answer to the best resampling strategy as well as the best spatial resolution is almost impossible because this answer is closely related to the questions asked by any stakeholder or decision maker.

GeoWEPP definitely offered a robust possibility for simulating soil erosion processes caused by water. This approach additionally provided the possibility for visualization of spatial erosion and deposition patterns. The underlying classification concept for this visualization, incorporating the tolerable soil loss value, adds a lot of flexibility in terms of decision making onto this tool. Various text output files of GeoWEPP provide additional information that support further analysis.

Despite the comfortable usability regarding the GeoWEPP soil erosion simulation approach, any model user should be aware of consequences on simulation results regarding spatial resolution of the used DEM. As shown in this study the spatial resolution of the used digital elevation model as

well as the selected resampling strategy showed noticeable influence on simulation results regardless of spatial scale of interest.

References

Boardman, J., in press: Soil erosion science: Reflections on the limitations of current approaches. Catena

Cochrane, T.A., Flanagan, D.C., 1999: Assessing water erosion in small watersheds using WEPP with GIS and digital elevation models (Fourth Quarter 1999), Journal of Soil and Water Conservation, 678-685

Cochrane, T.A., Flanagan, D.C., 2003: Representative hillslope methods for applying the WEPP model with DEMS and GIS, Transactions of the ASAE Vol. 46(4), 1041-1049

EEA, 2003: Environmental assessment report No. 10, European Environmental Agency, Kongens Nytorv 6, DK-1050 Copenhagen

Flanagan and Livingston, 1995, USDA – Water Erosion Prediction Project, NSERL Report No. 11, July 1995 National soil research Laboratory USDA-ARS-MWA 1196 SOIL Building, West Lafayette, IN 47907-1196

Flanagan, D.C., Nearing, M.A., 1995: USDA-Water Erosion Prediction Project (WEPP), NSERL Report No. 10, National Soil Erosion Research Laboratory, West Lafayette, Indiana 47907

Garbrecht, J., Martz, W.L., 1999: TOPAZ Overview, Rep.# GRL 99-1, Grazinglands Research Laboratory, USDA, Agricultural Research Service, El Reno, Oklahoma

Garbrecht, J., Martz, W.L., 1997: The assignment of drainage direction over flat surface in raster digital elevation models, Journal of Hydrology 193, 204-213

Golden Software, 2002. SURFER Version 8.02, Reference Manual Volume 1, Golden Software Inc., Colorado

Isaaks, E.H., Srivastava, R.M., 1989: An Introduction to Applied Geostatistics, Oxford University Press Inc, New York

Lal, R., 1997: Degradation and resilience of soils, Phil. Trans. R. Soc. Lond. B 352, 997-1010

Martz, W.L., Garbrecht, J., 1999: An outlet breaching algorithm for the treatment of closed depressions in a raster DEM, Computers & Geosciences 25, 835-844

Merritt, W.S., Letcher, R.A., Jakeman, A.J., 2003: A review of erosion and sediment transport models, Environmental Modelling & Software 18, 761-799

Nearing, M.A. 2006: Can soil erosion be predicted?, Chapter 6. In: Soil Erosion and Sediment Redistribution in River Catchments, P. Owens (ed.), CABI Publishing. p. 145-152.

Renschler, C.S., 2003: Designing geo- spatial interfaces to scale process models: the GeoWEPP approach, Hydrol. Process. 17, 1005-1017

Renschler, C.S, 2005: Scales and uncertainties in using models and GIS for volcano hazard prediction, Journal of Volcanology and Geothermal Research (139), 73-87